Demonstration of the Advanced Dynamic System Modeling Tool TRANSFORM in a Molten Salt Reactor Application via a Model of the Molten Salt Demonstration Reactor

M. Scott Greenwood†*

Benjamin R. Betzler†

A. Lou Qualls†

Junsoo Yoo‡

Cristian Rabiti‡

†Oak Ridge National Laboratory

‡Idaho National Laboratory

*Corresponding author

greenwoodms@ornl.gov

F: (865) 576-3513

1 Bethel Valley Rd

PO Box 2008, MS-6170

Oak Ridge, TN 37831-6170

Total pages: 54

Number of figures: 24

Number of tables: 14

Demonstration of the Advanced Dynamic System Modeling Tool TRANSFORM in a Molten Salt Reactor Application via a Model of the Molten Salt Demonstration Reactor[1]

M. Scott Greenwood, Benjamin R. Betzler, A. Lou Qualls, Junsoo Yoo, and Cristian Rabiti

Abstract

Liquid-fueled nuclear reactors, particularly molten salt reactors (MSRs), have recently gained significant interest in the advanced reactor community. As with all reactors, modeling and simulation are critical to advanced reactor design and licensing and will be required for MSR deployment. However, there are significant gaps in existing simulation capabilities for MSRs, particularly with the unique challenges of liquid-fueled systems (e.g., fission product transport). Furthermore, advanced reactor designers require near-term tools which are readily modifiable to perform design and analysis, including the ability to extend their analysis beyond the primary system to auxiliary systems. TRANSFORM, a Modelica-based, system modeling library developed at Oak Ridge National Laboratory (ORNL), is an advanced tool which can help meet some of the near-term needs of the advanced reactor community. This paper describes advanced system modeling criteria and presents TRANSFORM to the advanced reactor community by demonstration of system modeling capabilities and support of advanced analysis workflows, i.e., the RAVEN framework from Idaho National Laboratory, using the liquid-fueled Molten Salt Demonstration Reactor (MSDR) as a reference design.

Keywords

liquid-fuel molten salt reactor; system model; TRANSFORM; Modelica; sensitivity analysis; RAVEN

Demonstration of the Advanced Dynamic System Modeling Tool TRANSFORM in a Molten Salt Reactor Application via a Model of the Molten Salt Demonstration Reactor

I. Introduction

Recent years have seen a significant increase in the reactor community's interest in advanced reactor systems, specifically molten salt reactors (MSRs). As a broad class of reactors, MSRs have the potential to directly fulfill many US energy policy objectives of secure, affordable, and environmentally conscientious energy supply.[1–3] The number of possible salt and material combinations that can be used in MSRs leads to a broad range of potential MSR concepts. For a basic representation, MSRs can be classified into the following groups:

1. **Liquid-cooled reactors**, in which a solid fuel undergoes fission and is cooled by a separate non-fueled primary system salt. Also referred to as salt-cooled.
2. **Liquid-fueled reactors**, in which a flowing fueled salt contains fissile material that fissions when in the core and flows throughout the primary system, and possibly other auxiliary systems, serving as fuel and coolant. Also referred to as salt-fueled.

Both liquid-cooled and liquid-fueled concepts can be fast, epithermal, or thermal spectrum reactors, with the primary categories loosely defined as liquid-cooled fluoride, liquid-fueled fluoride, and liquid-fueled chloride-fast (Figure 1). Liquid-cooled concepts of current interest are mainly thermal spectrum concepts that use fluoride salts as the primary coolant. This class of reactor, known as fluoride liquid-cooled high-temperature reactors (FHRs), has been the subject of a significant amount of recent MSR research, including conceptual design studies at Oak Ridge National Laboratory (ORNL).[4–9] Because liquid-cooled reactors have a fixed fuel form, the analysis of their behavior and performance is expected to be more analogous to traditionally licensed reactor designs. Therefore, existing modeling and simulation capabilities (e.g., CASL, SCALE, RELAP, TRACE) are likely appropriate for many aspects of the FHR design and licensing process.[9] However, the nature of dissolved fuel in a molten salt concept introduces many unique challenges (e.g., fission product transport) for which traditional reactor design and analysis tools must be modified if possible, or new ones created.

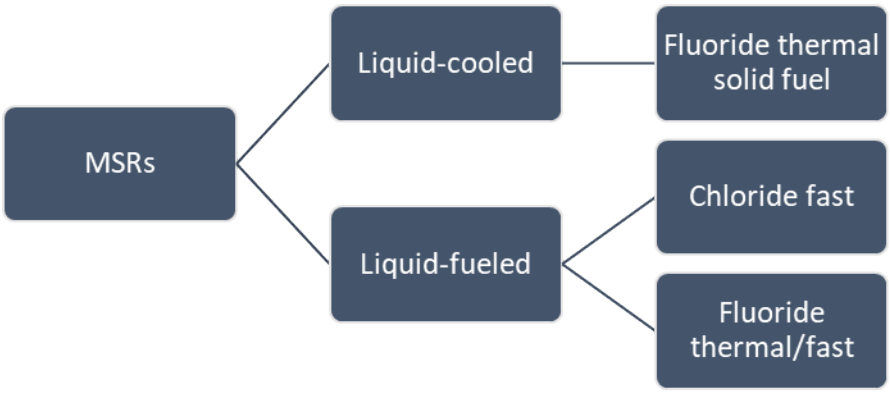

Figure 1. High-level categorization of MSRs.

The process to modify or create software, especially in terms of cost and time (often but not always interchangeable), is difficult to accurately predict.[10] To generate fully qualified software for nuclear licensing arguments is especially difficult and expensive given the requirements imposed for nuclear applications. For instance, one ongoing effort to provide a standard set of tools for the advanced nuclear community, the Nuclear Energy Advanced Modeling and Simulation Program (NEAMS), is expected to require a sustained minimum investment of 20 million US dollars per year alone[11]. In the context of thermal-hydraulic system modeling, the domain of this paper, similar initiatives to develop highly sophisticated and qualified code (i.e., decades of time and millions of US dollars) have, and continue, to be developed such as the many variations of RELAP[12]. These types of activities are valuable and necessary investments, but they do not inherently deliver on the immediate needs of the community, especially reactor designers, who need tools now to understand the merits of their systems, modify designs, drum up investment funds, and initialize informed discussion with regulators. Furthermore, it must not be forgotten that many of the state-of-the-art tools currently employed came into existence only after significant experience with light water reactor plants had been obtained; there was significant amount of verifiable data. MSRs on the other hand, even if one concept was selected, would still have a significant uncertainty in many key aspects of its behavior. It is difficult to properly design tools when much of the important phenomena are understood, even more so when so little data is available. This difficulty is greatly compounded when extended to the great variation of MSR concepts being explored. This discussion leads to the logical conclusion that there exists a gap between the immediate needs of the MSR community, the tools which will eventually be available, and the phenomenological

understanding which enables both community and tools to progress in a timely fashion. In order to bridge the identified gap, tools and workflows which rely on more flexible and open frameworks, while leveraging modern computational advancements, are required.

This paper presents one such tool, the Transient System Framework of Reconfigurable Models (TRANSFORM), using the Molten Salt Demonstration Reactor (MSDR) concept to demonstrate capability. The paper is an extension of an ORNL report[13] where additional details specific to the MSDR not contained in this article may be found. The paper will first provide a description of criteria needed from system-modeling tools for liquid-fueled MSRs, a summary of the TRANSFORM library and how it is able to meet the specified criteria, a description of the MSDR and associated TRANSFORM model including the motivation of its selection, and a few select steady-state and transient scenarios illustrating the ability of TRANSFORM to meet the specified criteria including an example of an advanced workflow using the Risk Analysis Virtual Environment (RAVEN) framework from Idaho National Laboratory.

II. System-Modeling Tool Criteria for MSRs

Model criteria establish the baseline information required to be returned from a tool in order to achieve one's goals. For example, it can be generally assumed that the goal of an advanced reactor designer is to be able to progress their understanding of their technology in a timely fashion such that it can ultimately be licensed by the appropriate regulatory bodies and approved for deployment. Furthermore, once a tool(s) is selected, criteria inform modeling decisions (e.g., reasonable assumptions, necessary components, phenomenon to investigate) which do not compromise the ability to properly analyze the system/scenario under investigation. Although, it is reasonable to assume that the criteria for various MSR technology will vary, it is equally clear that there exist common criteria for MSRs. The following sections outline topical area needs and associated criteria which system-modeling tools will need to address.

II.A. Licensing

US Nuclear Regulatory Commission (NRC) regulatory processes, of which licensing is one activity, are focused on fulfilling the mission to ensure the protection of public health, safety and the environment and to promote the common defense and security.[14] Without regulatory approval, a reactor technology

will not be deployed. Of primary importance in the NRC process are the types of radioactive sources and their pathways of exposure to site personal and the public. Current NRC regulations are predicated on nominally fixed fuel forms (i.e., encapsulated solid fuel that can be readily accounted for). Naturally, the unique nature of a dissolved fuel is beyond this assumption, and thereby in potential conflict with traditional NRC regulatory paradigms (e.g., source term accountancy). The precise regulatory language that will be adopted is an active area of research and investigation.[15] However, the need to account for the source terms in fulfilling the NRC's mission remains unchanged. How a liquid-fueled system behaves, the multiple locations of source terms outside the core, and the method for quantifying the movement of the source terms, including qualification under transient accident scenarios are examples of items likely needed to be addressed for any given reactor.[16] Questions required to be addressed by a technology include:

1. What are the lifecycles (e.g., birth, decay, reactivity) of the radioactive materials in the system?
2. What are the physical behaviors (e.g., transport, precipitation and/or plate out) of source terms?
3. Which source terms are important to safety analysis (e.g., dose)?
4. How can online refueling and/or salt processing mitigate excess reactivity concerns and/or potential accident consequences?

II.B. Safeguards

The International Atomic Energy Agency (IAEA) safeguards objective is specified in Paragraph 28 of INFCIRC/153 [17] as:

> *the timely detection of diversion of significant quantities of nuclear material from peaceful nuclear activities to the manufacture of nuclear weapons or of other nuclear explosive devices or for purposes unknown, and deterrence of such diversion by the risk of early detection.*

An effective safeguards system for MSRs requires a deep scientific understanding of change detection—a clear understanding of how the quantity, isotopic composition, and chemical/physical form of nuclear material changes with normal operational variations and anticipated operational occurrences. Furthermore, being able to clearly distinguish acceptable variations from changes due to nuclear material diversion scenarios is necessary to accurately detect undeclared activities via sensor integration at the system level.

A comprehensive safeguards approach has not yet been determined for MSRs. Even so, it is advisable to be proactive in addressing potential safeguards needs during the design phase rather than retrofitting the plant to incorporate safeguards after it is commissioned. A safeguards-by-design approach will be most effective. Some questions pertinent to addressing MSR safeguards are as follows:

1. What potential operations scenarios can change the amount of fissile material produced in an MSR, and what potential scenarios can change the quality and quantity of fissile material that is separated?
2. What signatures of off-normal changes vs. acceptable operational variations could indicate clandestine operations?
3. What are the interdependencies of the operational parameters and the resulting signatures?
4. Where must instruments be placed to detect these changes?

II.C. Agile Development

Agile development embraces a workflow of incremental progress through a parallel process of analyzing, designing, testing, and incorporating feedback. Some colloquial descriptions of the process include “fail fast” or the “minimally viable product (MVP)” idea. The original manifesto[18] and guiding principles[19] of the agile method include emphasis on ideas such as working software, collaboration, and responding to change. Flexibility and timeline are two concepts directly applicable to this agile method.

II.C.1. Flexibility

One of the defining characteristics of MSR technology is the great variety of systems that can be designed. As such, effective tools must allow the user to be able to readily introduce new features/methods into the tool or modify existing ones for their specific purposes. For example, a recent pre-phenomena identification and ranking table (pre-PIRT) report[15,20,21] highlighted areas such as composition tracking, thermophysical properties, heat transfer correlations, salt composition, corrosion, gas behavior (e.g., tritium), and extension to auxiliary systems as critical features for evaluating figures of merit of the liquid-fueled systems. These areas were noted as having a great deal of uncertainty and significant variability based on a specific design. Advanced tools will be expected to enable the user to have the freedom to efficiently modify and extend the system modeling tools to meet their needs, such as ability to vary the mentioned features and integrate with other tools and workflows (e.g., uncertainty analysis). A sharp contrast to traditional modeling paradigms.

II.C.2. Timeline

The nuclear community have recognized the need for a focused effort to provide modeling and simulation tools to accelerate and enable advanced reactor technologies. In this effort, programs (e.g., NEAMS[11]) are coordinating efforts to deliver suites of tools to achieve the required design and analysis to facilitate the delivery of licensable technology. However, these tools and workflows take significant periods of time and money in order to progress. Of the two, time is especially of concern given the significant amount activity in the advanced reactor space[22] and the prerequisite to meet energy demand in a world of evolving environmental and economic policies. While these organizations and the codes which will be under their umbrella are developed, the advanced reactor community requires tools today to make progress in testing theories, exploring feasibility and performance of ideas, and investigating and identifying important issues or system sensitivities. The information gleaned from these near-term tools will improve the more fully qualified tools which will serve as the approved approaches for establishing safety basis, permitting deployment of a given reactor technology.

II.D. Criteria Summary

The associated needs of licensing and safeguards, coupled with requirements for flexibility and near-term solutions, form a design envelope which guide the requirements of the advance reactor tools. Based on the previous discussion, a few criteria to be addressed by system-modeling tools for MSRs have been identified and are presented below. As applicable, the licensing (L#) or safeguards (S#) question to which the criteria broadly apply are provided. However, this assignment should be taken lightly. Just as MSR behavior is highly interwoven among the various physics, so are the methods needed to investigate them. Furthermore, it would be unreasonable to assume that this list exhaustively covers all things necessary for addressing licensing and safeguards needs for MSRs.[16] Still, these criteria represent an important baseline for advancing the understanding of, and conversation around, MSRs.

1. (L1, L2) Inclusion of delayed neutron precursor models that account for delayed neutron precursor production, transport, and decay throughout the primary fueled reactor loop (i.e., reactor core to primary heat exchanger and back) and auxiliary systems
2. (L2, S1) Radionuclide inventory accounting, including source term production and holdup and release mechanism models
3. (L4, S1, S2, S3) Thermal-hydraulic analyses of sufficient fidelity to capture flow and power dynamics in liquid-fueled concepts

4. (L3) Time-, temperature-, flux-, and flow-dependent materials and salt interaction data, and models to predict corrosion, erosion, and irradiation effects
5. (S4) Ability to integrate sensor location and performance into model behavior.
6. Ability to support an agile development workflow (e.g., flexibility and rapid prototyping).
7. Enables integration with other advanced tools and workflows

III. TRANSFORM

The Transient Simulation Framework of Reconfigurable Models (TRANSFORM) is a Modelica-based library developed at ORNL.[23] The tool's primary purpose is enable rapid development of dynamic advanced energy systems (nuclear and otherwise) via the establishment of a modern and extensible system modeling tool. Critical elements of this effort include (1) development of a library of baseline generic component models able to be assembled into a myriad of full system models using available geometry, design, and associated (i.e., thermal-hydraulic) data; (2) definition of modeling conventions for model and component development; and (3) establishment of user interfaces, support, and analysis tools to facilitate simulation development and analysis. TRANSFORM development is maintained internal to ORNL with a periodic open-source release hosted on Github.[2] TRANSFORM is currently developed using the commercial integrated development environment (IDE) Dymola[24] from Dassault Systemes but should be compatible with other IDEs which fully support Modelica Specification 3.4+.[25] A final note, TRANSFORM is not directly funded, rather its capabilities have been gradually extended as a by-product of curating work done for various projects into a reusable resource since its inception in 2015.[26–30] This paper simply represents research done in the area of MSRs and subsequently incorporated into TRANSFORM so that it may be reused for future studies.

TRANSFORM is organized as a series of packages each with a general application as specified by its name (Figure 2). Within each package, the library sub-categorizes models to assist the user in finding a component applicable to their task. Although many models are already available, the object-oriented nature of the programming language enables the user to view, extend, and/or modify (i.e., source code is accessible) any component at the level needed for the use case or add new models to TRANSFORM.

---

[2] https://github.com/ORNL-Modelica/TRANSFORM-Library

The user has complete freedom to adapt TRANSFORM to meet the needs of their specific project. Furthermore, the modeling conventions (i.e., fluid and heat connectors) adopted in TRANSFORM are also those accepted by the open-source community library, the Modelica Standard Library, allowing users to leverage many other open-source or private/commercial libraries as needed.

The following subsections provide a brief description of the Modelica language, an example of the replaceable or extensible nature of TRANSFORM, and a succinct description of trace substances—the method employed in TRANSFORM for tracking fission products for liquid-fueled MSRs.

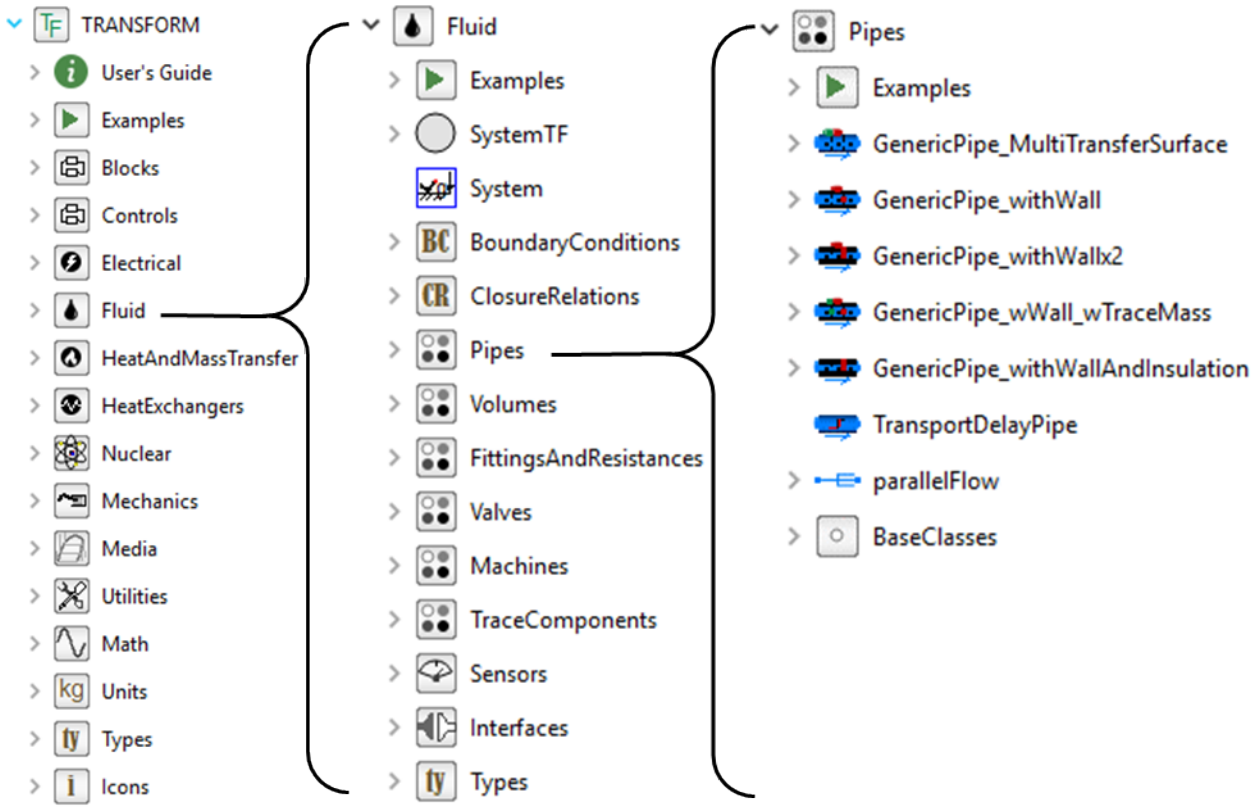

Figure 2. Existing layout of the TRANSFORM library and example of models within the 'Fluid' and 'Pipes' packages.

III.A. Modelica

Modelica[25,31] is a nonproprietary, object-oriented, equation-based programming language used to conveniently model complex physical and cyber-physical systems (e.g., systems containing mechanical, electrical, electronic, hydraulic, thermal, and control components). A visual representation of prominent

applications and domains for which Modelica has been used is shown in the 'wordcloud' based on all abstracts from the 12th International Modelica Conference where word size reflects usage frequency. The interested reader is suggested to view the freely available conference papers from the International Modelica Conference[3] to obtain a broader perspective of Modelica.

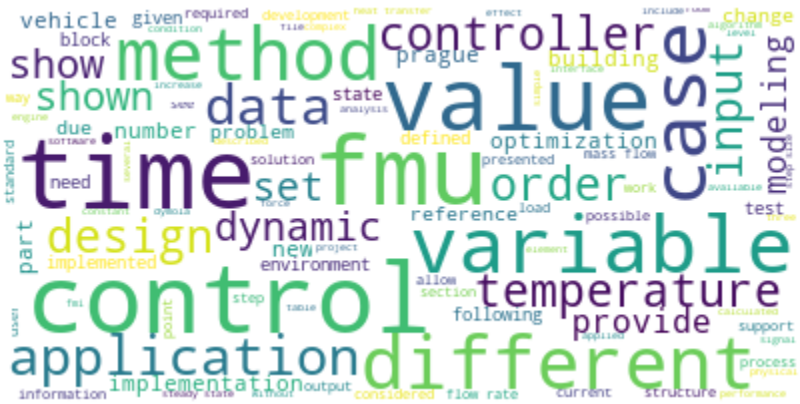

Figure 3. A 'wordcloud' created from the abstracts of the 12th International Modelica Conference demonstrating application areas of the Modelica programming language.

Two key advantages of Modelica are its separation of the development and solution process and the language formulation used (i.e., acausal, time-dependent, and object-oriented). While each of these items could be expounded upon at length, these points shall be briefly summarized in terms of some of the modeling criteria set forth in Section II.

III.A.1. Process Separation

Modelica divides the modeling process into compartmentalized steps: the physical model; the compiler; and the solver. This separation approach enables the physical model to be developed and used in any operating system (e.g., UNIX or Windows) or system configuration (e.g., server cluster or desktop computer) and allows for the user to select, or develop, a solver appropriate to their problem. This workflow also allows for the physical model to be readily integrated into other tools, with the

[3] https://www.modelica.org/publications/ModelicaConference

option to yield control over the solution process to that tool (co-simulation vs. model exchange). The compartmentalization of tasks and ability to integrate tools was one of the principle motivations for Modelica and is now a formal standard called the Functional Mock-up Interface (FMI), models exported using FMI are called Functional Mockup Units (FMUs – Figure 3).[32] There are many variations of how the FMI technology can be applied (e.g., supported by many tools such as ANSYS Simplorer and SIEMENS Amesim, see website for a full list[4]) but in regards to the criteria, a Modelica based modeling approach leverages a technology designed to interact with advanced tools and workflows.

III.A.2. Language Formulation

From its inception, Modelica was intended to enable systems of dynamic (i.e., time-dependent) or ordinary differential equations (ODEs) to be modeled efficiently. As such, the language adopted an acausal, object-oriented modeling approach. An acausal, or declarative language allows the computer to decide on the most appropriate algebraic manipulation to achieve a solution while freeing the user to only declare behavioral relationships. Colloquially, the modeler could code equations as they might appear in a textbook and the computer would determine how everything will be solved. This permits the modeler to focus on including and understanding the behavior characteristics (e.g., engineering) and minimize time spent rearranging and optimizing the forms of the equations into a solvable matrix, arguably a task better undertaken by a computer. Figure 4 provides a simple demonstration of this concept via the implementation of a classic ODE problem, the Lorenz System. The figure depicts the simplicity by which one can leverage these capabilities of Modelica to quickly generate the solution of a complex problem. This ability to focus on the problem in the natural context of the modeler's experience (e.g., mechanical or electrical engineering) and permit the computer to determine the solution process rapidly minimizes development time.

---

[4] https://fmi-standard.org/tools/

Math

$$\frac{dx}{dt} = \sigma(y - x)$$

$$\frac{dy}{dt} = \rho x - y - xz$$

$$\frac{dz}{dt} = xy - \beta z$$

Modelica

```
model LorenzSystem
  input Real sigma = 1;
  input Real rho = 1;
  input Real beta = 1;
  parameter Real x_start = 1 "Initial x-coordinate";
  parameter Real y_start = 1 "Initial y-coordinate";
  parameter Real z_start = 1 "Initial z-coordinate";
  Real x "x-coordinate";
  Real y "y-coordinate";
  Real z "z-coordinate";
initial equation
  x = x_start;
  y = y_start;
  z = z_start;
equation
  der(x) = sigma*(y-x);
  der(y) = rho*x - y - x*z;
  der(z) = x*y - beta*z;
end LorenzSystem;
```

Solution

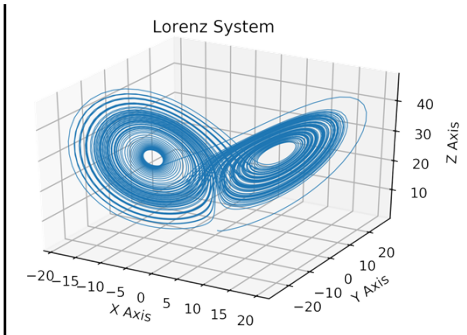

$$\sigma = 10; \rho = 28; \beta = 8/3$$
$$x(0) = 0; y(0) = 1; z(0) = 1.05$$

Figure 4. Simple example of the acausal, ODE solving capability of Modelica.

Applying an object-oriented approach enables an additional capability which is especially valuable in an advanced reactor modeling context. The ability to 'extend' or create 'replaceable' models. Given the uncertainty and variation in reactor systems, a modeler requires a natural means to experiment with different physics and component configurations. The Modelica language embraces and encourages the modeler to create increasingly complex components built upon simpler models via inheritance. TRANSFORM relies heavily on this capability. The reliance on inheritance allows generic models to specify the minimum information required, the inheriting model then providing additional information unique only to itself, thereby permitting a wide range of models to be accessible based on their common infrastructure. For example, Figure 5 demonstrates the graphical user interface (GUI) experience for modifying the heat transfer correlation of a pipe where the heat transfer correlation class is provided basic information from its instantiation in the pipe model (e.g., fluid state, pipe geometry, etc.), thereby creating a replaceable model. The user needs only to select their desired heat transfer model, if it does not already exist, and then re-simulate. No additional changes in the code structure or modification to any other underlying code is required.

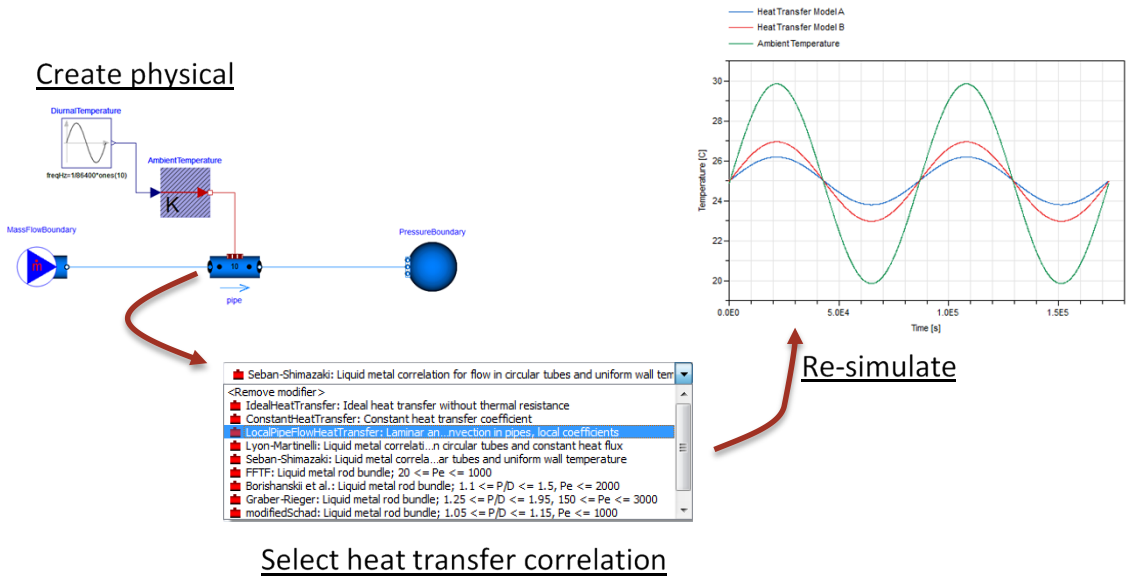

Figure 5. A model of a modification of the heat transfer correlation of a pipe subject to cyclic variations in ambient wall temperature demonstrating the object-oriented nature of Modelica enabling replaceable models.

III.A.3. Disadvantages of Modelica

There are many clear advantages in leveraging the modern programming language Modelica to create advanced system modeling tools. However, there are clear limitations of Modelica that should be mentioned related to 'solution control'. The workflow separation (i.e., model, compile, solve) inherently prevents a modeler from leveraging *a priori* knowledge of the model in creating custom control over the solution progress. Any special consideration of a tool or model would need to be handled by a custom solver developed specific applications.

Furthermore, modern mathematical approaches for parsing models and generating code that can be readily parallelize is an area of active research. The principle issue being that the domain neutral nature of Modelica requires solutions which do not depend on the application. To the author's knowledge, the ability to create efficient code for use on parallel infrastructures (e.g., high performance computing), free of application specific ties, has not yet been achieved (though embarrassingly parallel processes are commonly employed). This, and other considerations, naturally limit the size and complexity of problems for which Modelica is applicable (less than approximately 100,000 – 300,000 equations).[33]

Finally, the acausal approach of Modelica obscures the specific operations the computer is taking to arrive at a solution. In many ways creating a 'black box'. While it is extremely helpful to be able to quickly find solutions to complex problems, it also makes it extremely difficult to debug or otherwise analyze the solution process.

Other disadvantages may exist, but these are principle areas of concern, especially as the modeling community is pushing for larger and more complex systems which stretch the capabilities of Modelica. Fortunately, the Modelica language is being improved, via its specification and that of FMI, to incorporate the needs of the community. Also, the identified issues in large part are not language specific but IDE (e.g., Dymola). As the development environments and language advance, it is likely that these issues will be addressed, but for now they remain notable barriers to more complex and demanding projects.

III.B. Example Component: 'GenericPipe'

The MSDR model that will be described in Section IV relies almost exclusively on components contained within the TRANSFORM library. The interested reader is suggested to review the citations related to TRANSFORM and the TRANSFORM source code to better understand the implementation of any particular component. However, to assist the reader in better understanding general foundations of the MSDR model, a brief description of the underlying equations of the pipe model used in both the primary fuel and coolant loop is presented.

The pipe component used in the model of the MSDR is the 'GenericPipe_MultiTransferSurface' model (Figure 2). 'Generic' refers to the ability of the pipe to be modified for numerous applications and 'MultiTransferSurface' indicates that the user can specify multiple surface by which heat and/or mass transfer with the fluid may occur, such as in annular tube-type geometries. This component is a modified version of the 'DynamicPipe' included with the Modelica Standard Library[34], a 1D homogenous equilibrium model. The governing equations for mass, energy, and momentum are shown in Eqs. (1–4).

$$\text{Mass: } \frac{\partial(\rho A)}{\partial t} + \frac{\partial(\rho A v)}{\partial x} = 0 \tag{1}$$

$$\text{Momentum: } \frac{\partial(\rho A v)}{\partial t} + \frac{\partial(\rho A v^2)}{\partial x} = -A\frac{\partial p}{\partial x} - F_F - A\rho g\frac{\partial z}{\partial x} \tag{2}$$

$$\text{Energy: } \frac{\partial(\rho A u)}{\partial t} + \frac{\partial(\rho A v(u + p/\rho))}{\partial x} = -vA\frac{\partial p}{\partial x} + vF_F + \frac{\partial}{\partial x}\left(kA\frac{\partial T}{\partial x}\right) + \dot{Q} \tag{3}$$

$$\text{Pipe friction: } F_F = \frac{1}{2}pv|v|fS \tag{4}$$

where x is the spatial coordinate of flow, t is time, v is velocity, T is temperature, p is pressure, ρ is density, u is specific internal energy, z is elevation, A is the area perpendicular to the direction x, g is gravity, f is the fanning friction factor, S is the pipe circumference, and $\dot{Q}$ is heat transferred to/from the fluid.

The model is implemented using a finite volume method and a staggered grid scheme for the momentum balances. The closure relationships for geometry, heat transfer, and friction model are implemented using replaceable models, allowing the modeler to select, or add, the appropriate method for their application. The default selections for each model are as follows: geometry = straight pipe; heat transfer = ideal; friction model = Colebrook-White (Turbulent) and Hagen-Poiseuille (Laminar) using a hyperbolic tangent sigmoid based on Reynolds number to smooth the transition between the regions. A recommended document for additional details on fluid modeling in Modelica is presented by Casella, et. al. (2006).[35]

III.C. Trace Substances: Fission Product Accountancy

For many aspects of licensing and safeguards of liquid-fueled reactors, as identified in Section II, it is necessary to have a means to account for fission product movement and holdup within the system. This accountancy enables estimations of important aspects of safety analysis such as dose or decay heat. The means by which TRANSFORM tracks fission products as well as other substances of interest is via a trace substance approach. Trace substances (C) are tracked as mass-weighted fractions of the primary flow ($\dot{m}$). They flow as a homogenous part of the primary fluid, but do not participate in the normal mass balance of the primary fluid. In this way, trace substances are carried along by the primary fluid wherever it travels. For example, Figure 6 illustrates the nominal behavior of trace substance flow ($\dot{m}_C$) in relation to the primary fluid. If off-nominal flow schemes are desired, such as accounting for separation efficiencies of a mechanical or chemical process, additional models may be introduced into the TRANSFORM model to capture the desired physics. The trace substance approach enables capture of the important aspects of dissolved fuel while minimizing additional unnecessary complexities (e.g.,

complex media property). For a more detailed discussion of trace substances the reader is directed to Greenwood and Betzler (2018).[36]

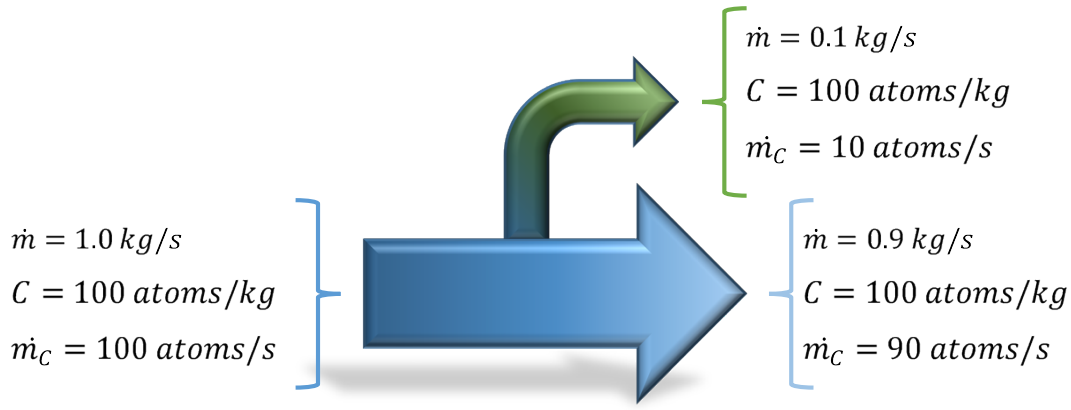

Figure 6. Trace substance flow ($\dot{m}_C$) behavior dependency on primary flow rate ($\dot{m}$).

IV. Molten Salt Demonstration Reactor

Phenomena identification and development and the actual implementation of that information into a working system model are two distinct tasks. From the author's experience, the complications of integrating phenomena into models is largely neglected, unfortunate given the degree of difficulty it can impose. There is significant value in proving out the entire workflow to ensure a complete understanding of necessary information for implementation as well as impact on model behavior and structure. The sooner this information is known the better it can be maturely integrated into future tools. Therefore, development of a physics-based system-level model of a liquid-fueled MSR, leveraging existing capability of TRANSFORM, was identified as a high-impact, low-cost task. The system model will enable progress in areas such as sensitivity analysis of parameters (e.g., heat and mass transfer coefficients) and exploration of safeguards and nuclear material accountancy. For example, this work has already enabled the development of a modified point kinetic model for a liquid-fueled system, including the impact of fission product transport via a trace substance approach, reactivity feedback, and decay-chain considerations.[36]

IV.A. Why model the MSDR?

The Molten Salt Demonstration Reactor (MSDR)[37] was chosen as the base design concept for the fluoride liquid-fueled reactor dynamic model (Figure 7), as it is based on publicly available documentation, of a power level on par with modern designs under development, and features important auxiliary systems such as off-gas, decay heat removal, and power conversion systems. Furthermore, the original goal of the MSDR design was to demonstrate the molten-salt reactor concept on a semi-commercial scale while minimizing development of basic technology beyond that already demonstrated by the Molten Salt Reactor Experiment (MSRE). This philosophy in the MSDR design is mirrored in modern many modern MSR concepts meaning that the MSDR is many of the features and systems of the MSDR will likely be analogous to modern designs. A summary of the high-level design parameters of the MSDR is provided in Table 1 and a flow diagram of the portions of the MSDR included in the MSDR model are shown in Figure 8. Of note is that the original MSDR design was based on a Th-fueled salt while this study chose a U/Pu fuel salt. However, this choice can be easily modified in the future for alternative studies as necessary.

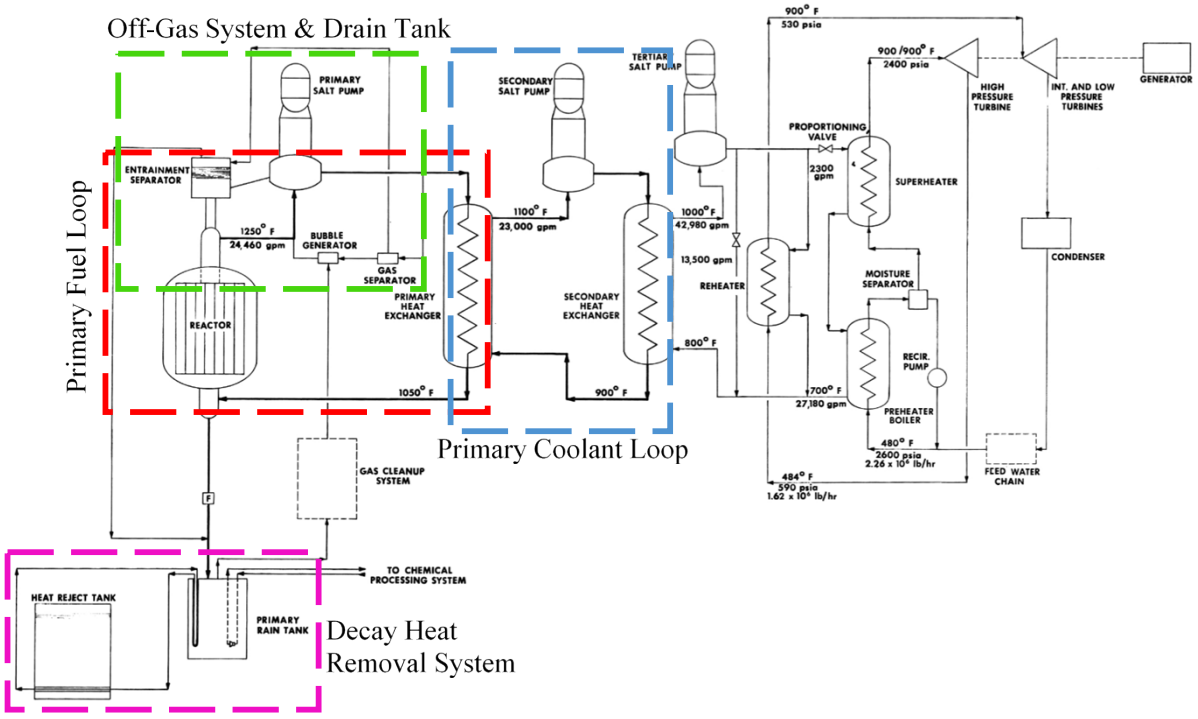

Figure 7. Flowsheet of the liquid-fueled thermal MSDR as taken from historical documentation.[37] Boxes represent corresponding systems between the MSDR flowsheet and the system model.

Table 1. Nominal design parameters of the MSDR

Parameter	Value
Thermal Power Rating (MW)	750
Operating pressure (MPa)	0.1
Salt type	$LiF\text{-}BeF_2$
Fuel type	U/Pu
Primary hot/cold leg temperature (°C}	677/566
Secondary hot/cold leg temperature (°C}	593/482
Primary total mass flow rate (kg/s)	5000
Secondary total mass flow rate (kg/s)	2800
Vessel/piping Material	Alloy-N
Nominal piping diameter (in/cm)	12/15.24
Nominal piping thickness (in/cm)	~0.5/1.27
Number of heat exchanger loops	3
Number of heat exchangers per loop	2
Total volume for graphite (m^3)	373
Total mass for graphite (kg)	662440
Primary total salt volume (m^3)	41
Secondary total salt volume (m^3)	43
Primary total salt mass (kg)	138540
Secondary total salt mass (kg)	87760
Pipe Length (m): A → B	6
Pipe Length (m): B → A	17.4
Pipe Length (m): B → C	7
Pipe Length (m): C → B	6.4

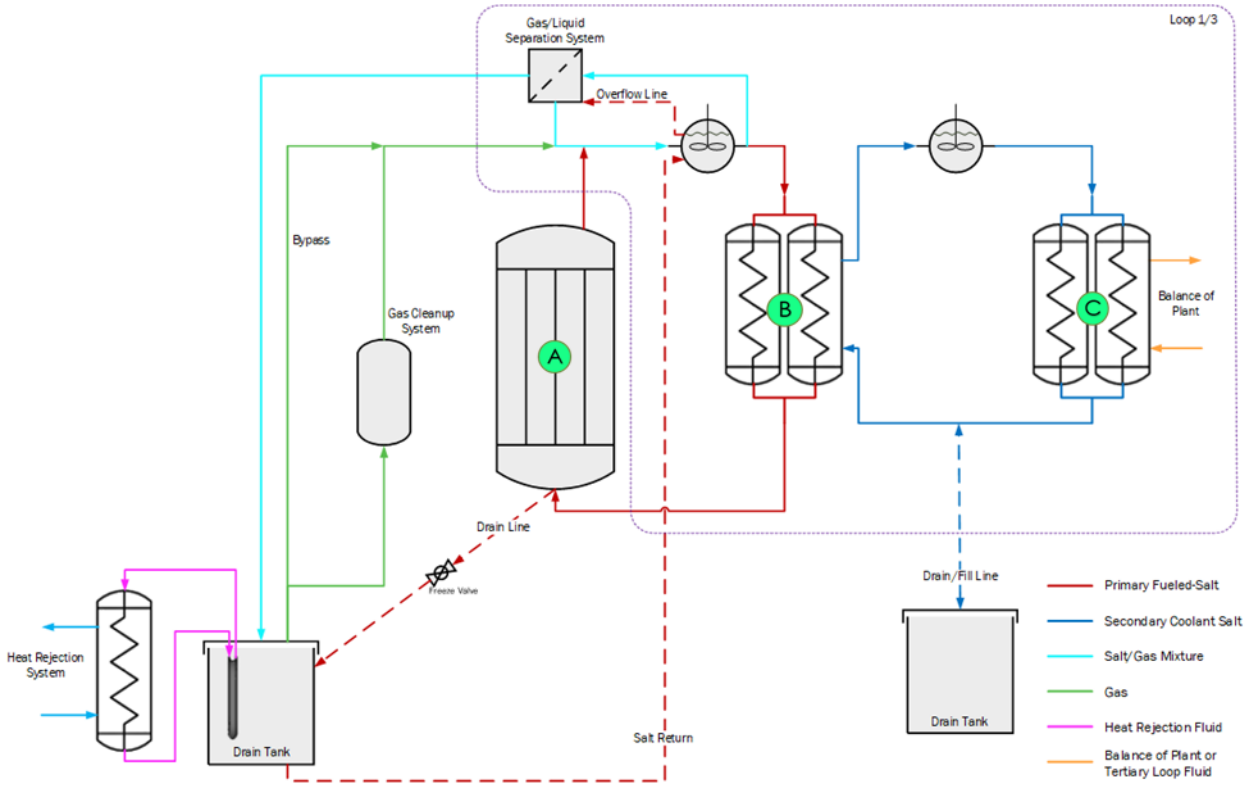

Figure 8. Simplified flow diagram of the components modeled in the MSDR.

An advantage of basing the reactor concept on an existing design like the MSDR is that the detailed design document was developed by researchers who were intimately familiar with the MSRE technology. The MSDR also leverages the work of the carefully documented MSBR[38] for information on off-gas, chemistry, materials, neutron physics, fuel reprocessing, etc. This model provides information that directly applies to the development of commercial reactors, minimizing development requirements and systems complications.

The system model (Figure 9) was developed based on the available MSDR literature and the identified criteria. Specific subsystems and other important phenomena are discussed in more detail below. Other critical systems that impact the reactor behavior, such as the balance of plant (BOP), will be modeled in the future. Additional information on the various components and subsystems (e.g., detailed dimensions) can be found in Greenwood et al.[13]

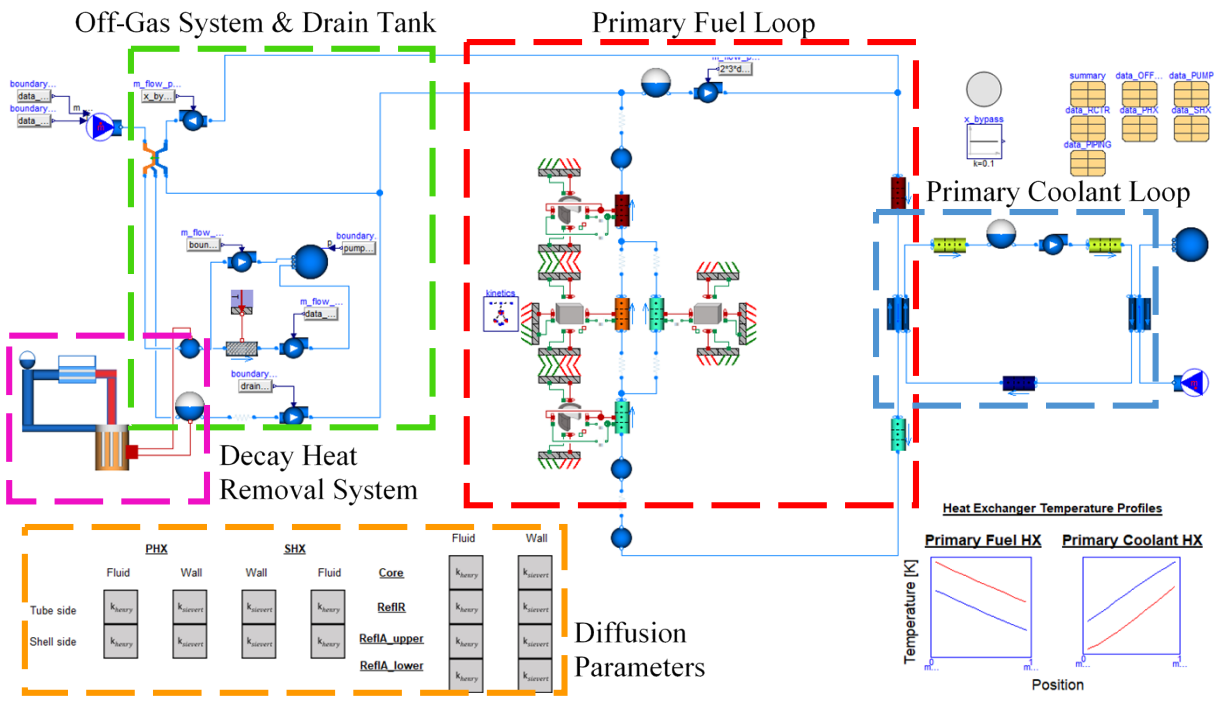

Figure 9. System model of a fluoride salt–fueled thermal reactor based on the MSDR. Boxes represent corresponding systems between the MSDR flowsheet and the system model.

IV.B. Primary Fuel and Coolant Loop

The primary fuel loop (PFL) is defined as the primary circuit of fuel salt, including the reactor, the primary fuel pump, piping to and from the primary heat exchanger, and the primary heat exchanger (fuel side). The principal component of the PFL is the reactor (Figure 10). The reactor consists of an inlet and outlet plenum, two axial reflectors, a radial reflector, and the core. Since the surface area and volume of graphite and fuel salt are important not only for heat transfer considerations but also for interaction with trace substances, a concerted effort was made to preserve reactor geometries in the model.

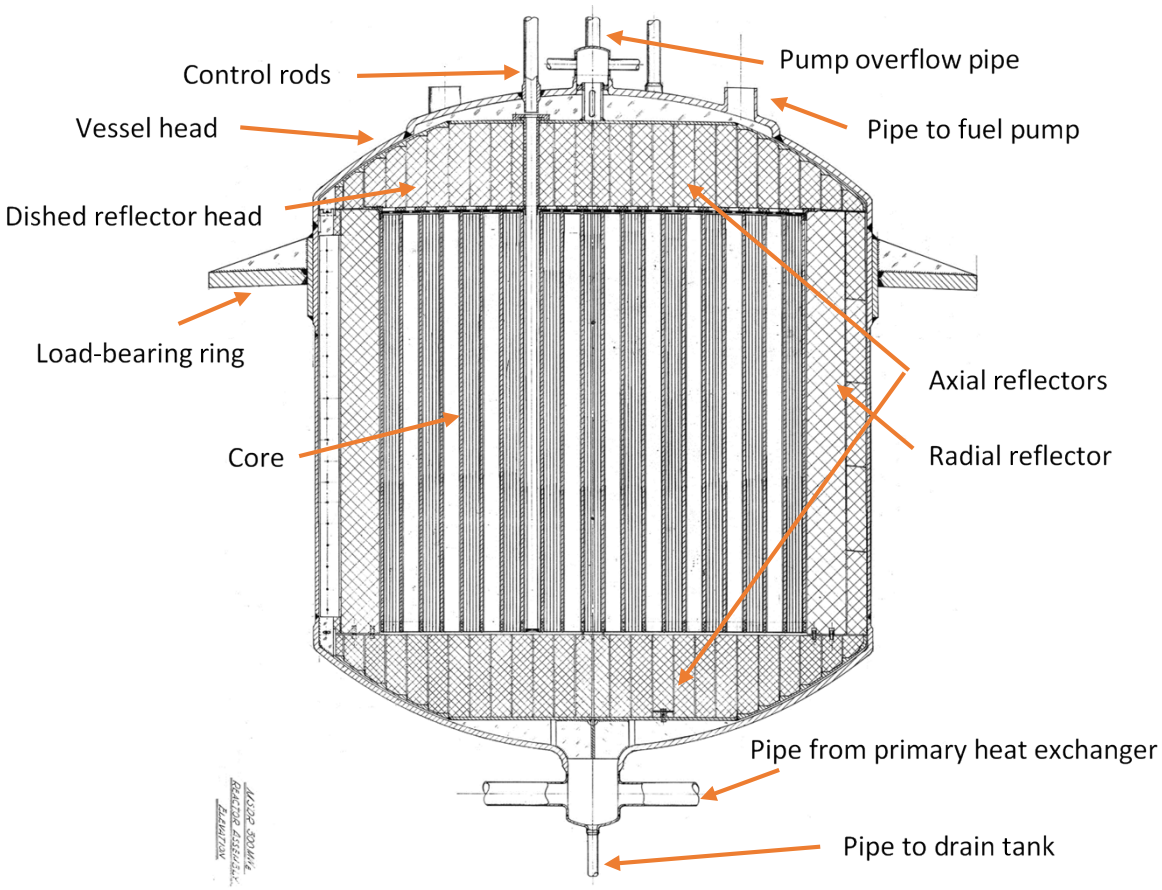

Figure 10. MSDR reactor vessel geometry (Bettis, Alexander, and Watts 1972, Fig. 2, ORNL DWG 72-2829).

The identical inlet and outlet plenums are ideally mixed volumes. The identical inlet and outlet graphite reflectors are made from radial rings of graphite, with each ring consisting of several smaller sections of graphite. The graphite is modeled as a 2D, 2nd order finite difference radial (r-z) conduction model with a specified number of parallel graphite blocks. Heat and mass transfer are modeled on the inner and outer radial surfaces and neglected on the top, bottom, and edge. The fluid subchannel is represented by a 1D discretized homogeneous fluid, with geometry specified by the total cross section area and the wetted perimeter of the reflector.

The radial reflector consists of stacked rectangular slabs and is likewise modeled with a 2D, 2nd order finite difference conduction model though using a slab (x-z) geometry instead of a radial geometry. The slab is assumed to have an adiabatic centerline which permits modeling only half of the slab thereby minimizing computational burden. However, to ensure the overall transfer balances are correct, the

number of parallel characteristic slabs is increased by a factor of two. Heat and mass transfer (e.g., tritium diffusion) are neglected on the top, bottom, and small edge of the block as the associated contribution to heat/mass transfer from these surfaces are very small compared to main face of the slab. The core region graphite (Figure 11) is also modeled with a 2D slab (x-z) conduction model with appropriate dimensions. The fluid channel was determined by the cross-sectional flow area and the wetted perimeter, in association with their respective graphite. In the figure, the outer gray structure and the red rectangular shaped objects are graphite. The salt flows in the small channels between the graphite where the black dots represent spacers to control graphite location.

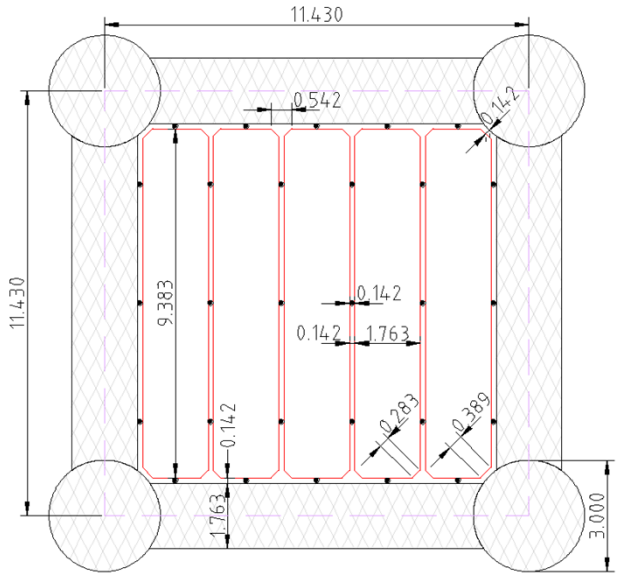

Figure 11. Reproduction of a core cell (Bettis, Alexander, and Watts 1972, Fig. 7; ORNL DWG 72-2830) (dimensions in inches); the dashed magenta line indicates a unit cell.

The pipes to and from the primary fuel heat exchanger dimensions are approximated based on rough estimations from drawings, as their dimensions were not specified in available documentation. Likewise, the pump and pump bowl were never fully defined, so the dimensions of the pump bowl were assumed to be like those of the MSBR. The off-gas system interfaces with the primary loop at the pump bowl inlet and the pump outlet by cycling a fraction of the overall primary salt flow through a separator to strip fission products (e.g., xenon gas) using a helium carrier gas. The diverted salt is then returned along with the nonseparated fission products to the pump bowl. A small amount of fuel salt taken with the carrier gas also leaves the system and travels to the drain tank, where it is then pumped back to the

pump bowl. The amount of salt sent to the drain tank and back to the pump bowl depends on the flow rate of carrier gas for the off-gas system and the level controls of the drain tank pumping system. The off-gas and drain tank systems are discussed in greater detail in Section IV.E.

The primary heat exchange rejection is via three salt loops, each with 2 parallel shell-and-tube heat exchangers (six heat exchangers in total).[37] Each set of primary heat exchangers reject heat to a primary coolant loop (PCL), whose salt is the same as the primary system without the dissolved fuel (i.e., FLiBe). The PCL is defined as the primary circuit of coolant salt, which includes the primary heat exchanger (coolant side), the coolant pump, the secondary heat exchanger (coolant side), and associated piping. Each of the three PCLs rejects heat to the BOP, which has been left as boundary conditions of a supercritical water cycle. Detailed summaries of the physical parameters for the primary fuel and coolant loops are given in Greenwood et al. (2018).[13]

IV.C. Reactor Kinetics & Fission Product Transport

The reactor kinetics implementation is a critical component of the system model, as it determines the reactor power output and establishes the behavior of the source terms (generation, reactivity feedback, etc.) throughout the system. The current implementation is based on a modified form of the point reactor kinetics[36] which treats the fission products as trace substances transported at the same rate as the primary carrier fluid, as described previously. This model captures the creation, decay, and transport of fission products and the reactivity feedback of neutron absorbers such as xenon, and it includes decay heat in terms of the near- and far-field energy deposition associated with fission products. Both precursor groups and other fission products are treated as trace substances and their behavior is tracked for all fluid volumes throughout the entire system.

IV.C.1. Precursor Groups

Parameters for the point kinetics model are shown in Table 2 from Betzler et al.[39] where i is the precursor group, λ_i is the decay constant, α_i is the normalized precursor fraction (i.e., $\beta_i = \alpha_i \beta$), and β is the effective delayed neutron fraction, and Λ is the prompt neutron generation time. The temperature reactivity feedback in the core (ρ) is driven by the fuel salt and the graphite (Table 3). In this paper, though not a limitation of TRANSFORM, it is assumed that the feedback from each fluid volume

contributed equally (i.e., no weighting factors) to the reactivity feedback of the fission power. The feedback parameters were taken from Robertson's ORNL-4541 report.[38]

Table 2. Summary of neutron precursor group parameters

Parameter	Value
λ_i (s^{-1})	0.0125,0.0318,0.109,0.317,1.35,8.64
α_i (-)	0.0320,0.1664,0.1613,0.4596,0.1335,0.0472
β (-)	0.0065
Λ (s)	1e-5

Table 3. Core temperature feedback parameters: $\boldsymbol{\rho = \alpha(T - T_{reference})}$

Parameter	Value
Type	Fuel salt, graphite
$T_{reference}$(°C)	649.114, 649.385
α (K^{-1})	-3.22e-5, 2.35e-5

IV.C.2. Fission Products

In addition to the precursor groups, a set of fission products are also tracked. In its current form, a full isotopic vector of over 2,200 nuclides is not a feasible for implementation due to the computational burden on the system model it would impose. . Instead, using a replaceable model structure which would allow for alternative selections to be made, a reduced set of isotopes was generated using ENDF-VII.1 data.[40] For this demonstration is was decided to filter and collect isotopes into groups representative of both the energy and time release of decay heat energy.

The reduction process yielded 25 fission product groups. Group decay constants and Q values were calculated by weighting the data by the independent yield of the constituent fission products. The sum of the constituent yields became the yield of a given group. For simplicity, the shortest-lived fission product group decays into the next shortest fission product group with the same constituent elements. While this is not physically true in all cases, this served as a simple model for demonstration purposes. Due to their importance in reactivity feedback and source term characterization, four isotopes are not grouped with the others: ^{135m}Xe, ^{135}Xe, ^{136}I, and ^{3}H. Future efforts may be made in expanding the number of groups able to be handled or couple with a depletion tool such as ORIGEN.

IV.D. Tritium Transport

The principle source of tritium in a system using FLiBe as the carrier salt is from neutron interaction with the FLiBe.[41] The major production pathways of tritium in a FLiBe-based system are shown in Eqs. (5–8). The generation rate of tritium is a function of the fission power and the cross section for tritium generation. Based on this interaction and the absorption of neutrons, the composition of the carrier salt changes with time (i.e., change in ^{6}Li and ^{7}Li) from a specified initial state. This change over time is captured in the model in a manner similar to other fission products as described in Greenwood et al.[36] The initial state of the a LiF-BeF_2 (67–33 mol %) carrier salt was 99.995% enriched in ^{7}Li.

$$^{6}_{3}Li + {}^{1}_{0}n \rightarrow {}^{4}_{2}He + {}^{3}_{1}H \tag{5}$$

$$^{7}_{3}Li + {}^{1}_{0}n \rightarrow {}^{4}_{2}He + {}^{1}_{0}n + {}^{3}_{1}H \tag{6}$$

$$^{9}_{4}Be + {}^{1}_{0}n \rightarrow {}^{6}_{2}He + {}^{4}_{2}He \tag{7}$$

$$^{6}_{2}He \rightarrow {}^{6}_{3}Li + e^{-} + \overline{v}\left(t_{\frac{1}{2}} = 0.8sec\right) \tag{8}$$

Tritium differs from other fission products due to (1) its generation by interaction of salt with neutrons, and (2) the manner in which it readily diffuses through piping at the elevated operating temperatures of MSRs, especially through the thin walls of the heat exchangers.[42] Using mass transfer analogies to heat transfer and Henry/Sieverts interface conditions between the salt and solid, Eqs. (9–12), the tritium is permitted to flow from the PFL to the primary coolant loop and from the primary coolant loop to the BOP through the respective heat exchangers. Transfer from the primary coolant to graphite in the reactor core also occurs using the same approach. Further details on the methodology can be found in Rader et al.[43] It is worth noting that the temperature dependence of the behavior of tritium (e.g., solubility in the salt and diffusivity in metal) is incorporated in this methodology. Other major components accountable for tritium leaving the PFL, or tritium management systems, may be incorporated in the future.

$$D_{ab} = D_{ab0} e^{-E_a/RT} \tag{9}$$

$$\frac{C_{salt}}{k_H} = \left(\frac{C_{solid}}{k_S}\right)^2 \tag{10}$$

$$k_H = k_0 e^{-BT} \tag{11}$$

$$k_S = k_0 e^{-\Delta H/RT} \tag{12}$$

where D_{ab} is the diffusion coefficient, R is the universal gas constant, T is temperature, C_{salt} and C_{solid} is the concentration of the substance in the respective body, and k is the solubility coefficient in the solid (k_S) and the fluid (k_H). D_{ab0}, E_a, k_0, B, and ΔH are constants as defined in Greenwood et. al. (2018).[13]

One important behavior specific to tritium is the relationship between chemical forms (i.e., T_2 and TF). An approach to account for the relation of chemical forms for tritium is outlined by Olander[44] and summarized in Zeng et al.[45] and Stempien.[41] In the current implementation of tritium tracking, tritium is not differentiated by its chemical form. However, the framework allows for this to be readily accomplished with minor modifications and may be performed as part of future work.

IV.E. Auxiliary Systems

Like any industrial scale facility, an actual MSR will have many auxiliary systems. Three systems important to MSRs that are included in the system model are the off-gas system, the drain tank system, and the decay heat removal system. While these systems are important for understanding performance and source term behavior, they are not well defined in literature. Therefore, engineering judgment and simplifications were made for preliminary modeling purposes.

In the model of the off-gas system, specified fission products (i.e., gaseous products) are removed from the primary fuel salt pump bypass line at a specified efficiency using a helium carrier gas (Figure 9). A portion of primary fuel salt which passes through the separator is carried to the drain tank at a rate dependent on the carrier gas flow rate. This salt is pumped from the drain tank back to the pump bowl of the PFL. The rate of fuel salt return from the drain tank can be controlled using the control settings of

the drain tank sump pump. The carrier gas with the separated fission products also travels to the drain tank. The characteristic hold-up time of the gas depends on the tank volume. From the drain tank, the gas is split at a specified ratio between a return line that runs directly back to the pump bowl and a charcoal adsorber bed. As the gas passes through the charcoal bed, substances decay, give off heat, and may become trapped. After exiting the charcoal bed, the carrier gas, along with any remaining substances that did not completely decay or that were otherwise filtered, are returned to the pump bowl.

The charcoal bed transports [46] the trace substances between volumes in the adsorber bed at a rate ($\dot{m}_C$) which is a function of the inflow rate, the time spent in a volume (τ), the decay rate of the substance (λ), and any sources of each substance from the decay of other substances, as shown in Eq. (13):

$$\dot{m}_{C,out} = \dot{m}_{C,in} e^{-\lambda\tau} + \sum \dot{m}_{C,decay} \tag{13}$$

The adsorber bed is heated by the decay of fission products. Like the drain tank heat removal system, the adsorber bed is cooled by a passive circulation loop. For simplicity, a fixed boundary temperature is set for the adsorber bed so that the cooling requirement can be easily monitored, as no design information is available for that system.

The drain tank is separated into two volumes (Figure 9), one for the gas and one for the fuel salt. The gas volume is determined by the liquid level of the fuel salt in the specified geometry, while the pressure of the fuel salt volume is set by the gas volume. Products decay and emit heat in each of these volumes and then continue through the process. The gas volume continues to the adsorber bed or goes directly to the pump bowl as previously discussed, while the fuel salt is pumped back to the pump bowl based on the control algorithm implemented. The preliminary control is a level monitor which switches its control setting based on minimum and maximum fuel salt levels. The drain tank is thermally connected with the decay heat removal system through double-walled thimbles, as described below.

The decay heat removal system (Figure 12) is a passive, buoyancy-driven, NaK-filled circulation loop. The loop removes heat from the drain tank via double-walled thimbles, which rely on radiation heat transfer between the pipes and convective heat transfer between the working fluids and the pipe walls.

The hot fluid rejects to a water tank at a higher elevation via identical double-walled thimbles. The cold fluid recirculates back to the drain tank to be reheated. Since this system is not well defined, a flow resistance is inserted into the loop so that the mass flow rate matches the design references. Physically, this resistance would be comprised of bends, orifices, and other pressure losses not already accounted for by the pressure drop correlations in the pipes. The water tank has a simple control system that maintains the outlet temperature at the design condition. The current model of the water tank includes a simple, ideally mixed volume that does not consider latent heat effects, so the flow rate required to keep the tank at design conditions is overestimated.

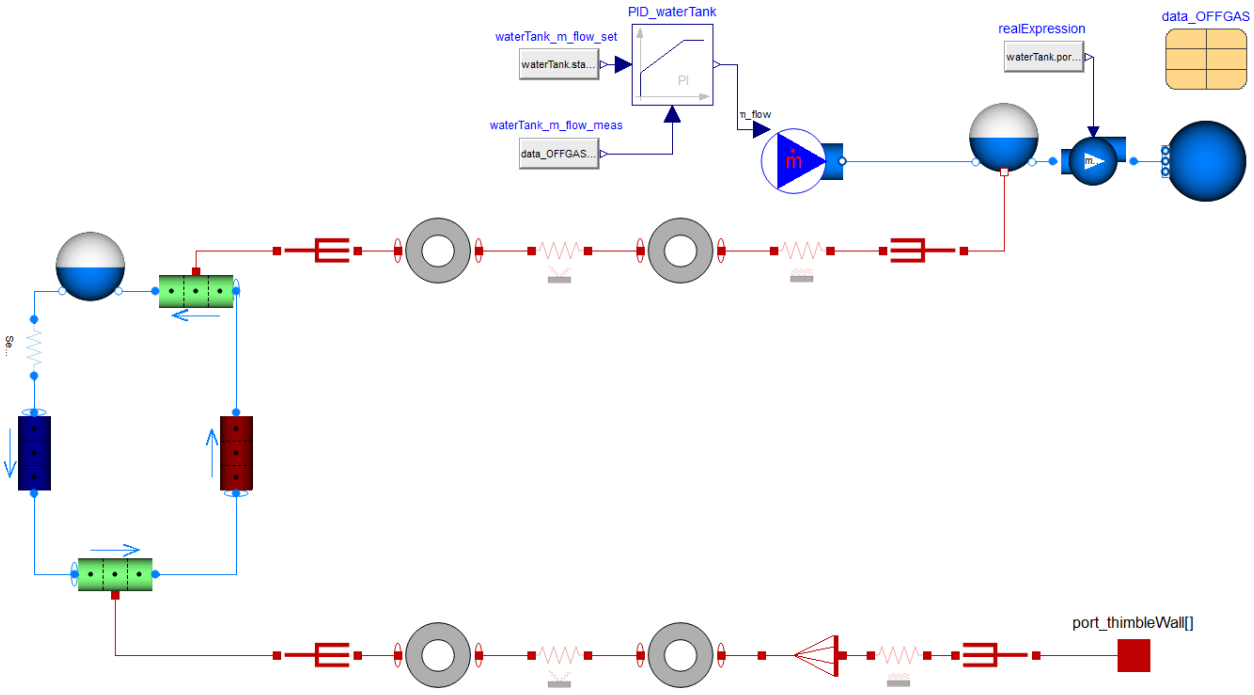

Figure 12. Model of the drain tank's natural circulation decay heat removal system.

IV.F. Closure Relations and Thermophysical Properties

Complex models require a variety of closure relations (i.e., pressure loss, heat transfer, and mass transfer correlations) and thermophysical properties which define the various materials and media of employed in the model. Specific details of all relations and properties can be found in Greenwood et al.[13] However, general correlations such as the Colebrook-White correlation for pressure loss and the

Dittus-Boelter correlation for heat transfer are used in the current model. As with most components, the chosen correlations can be updated as needed.

The thermophysical properties of the salt are worth special mention. The primary fuel and coolant salt are both modeled as a linear compressible FLiBe. The linear compressible fluid model indicates that the density is a linear function of temperature and pressure and assumes the following:

- The specific heat capacity at constant pressure (c_p) is constant
- The isobaric expansion coefficient (β) is constant
- The isothermal compressibility (κ) is constant
- Pressure and temperature are used as states
- The influence of density on specific enthalpy (h), entropy (s), inner energy (u), and heat capacity (c_v) at constant volume is neglected.

Important aspects of the linear compressible fluid model include the assumption of constant c_p and that the current implementation does not account for time-dependent fluid property changes based on items such as fuel burnup and fuel composition. As it is an area of active research, the measurement of thermophysical and transport properties of salts—especially with dissolved fuel—and their conversion to a functional database, [47] it is expected that these assumptions will be relaxed once property databases become available.

V. Results

There are many various accident and operation mode scenarios of potential interest to the regulator body and the MSR community. To present functionality of the model, three scenarios are presented. The first scenario allows the reactor to achieve a steady-state. Note that in an MSR, there is no true steady-state, so within the context of this report, *steady-state* refers to a condition in which fast evolving transients have died out, leaving only slowly changing effects such as the results of very long-lived fission products. This steady-state case also serves as the initial condition for the transient scenarios. The second scenario is a sensitivity analysis of several model parameters and consideration of how those parameters alter the baseline steady-state. The third scenario represents potential control and accident scenarios involving control rod operation and primary fuel pump trips. The same simulation setup was used for each scenario as is summarized in Table 4.

Table 4. Simulation setup summary for both steady-state and transient scenarios

Parameter	Value
Simulation Time (s)	172800
Real Time (s)	260
Solver	Esdirk45a
Solution tolerance	0.0001
Equations	13290

V.A. Steady-State

A steady-state condition was reached by simulating the model for 172,800 seconds (2 days). The extensive simulation time was due to permitting the reactor to start from zero concentration fission product; enough time was required for longer lived products such as xenon (half-life on the order of 9 hours) to build up to equilibrium concentrations. This section presents selected parameters of the model operating at a steady-state condition. All transient scenarios are initialized from the result of this simulation. A small selection of available steady-state variables is presented in Table 5 – Table 9.

Table 5. Steady-state inlet and outlet temperature of principle components (°C)

	Inlet	Outlet
Reactor	564.6	674.6
Core	564.6	683.0
Reflector	564.6	564.8
PHX PFL side (tube)	662.8	564.2
PHX PCL side (shell)	493.0	592.4
SHX PCL side (shell)	583.2	482.9
SHX BOP side (tube)	434.4	540.6
Drain tank	674.6	451.0

Table 6. Steady-state average core and reflector temperatures (°C)

		Average	Max	Min
Core	Salt	629.4	683.0	576.4
	Graphite	629.6	682.9	576.4
Reflector	Salt	564.7	564.8	564.6
	Graphite	564.7	564.8	564.6

Table 7. Steady-state flow rates and loop transit times

Variable	Value
PFL $\dot{m}$ (kg/s)	5,544
PCL $\dot{m}$ (kg/s)	2,797
PFL τ (s)	25.08
PCL τ (s)	31.37

Table 8. Steady-state power distribution (MW)

Variable	Value
Fission	724
Decay-heat (core only)	11
Decay-heat (loop and reflector)	7
Drain tank	2.5
Charcoal bed (kW)	394

Table 9. Tritium generation and release rate (atoms/s)

Variable	Value
Generation	3.6E+16
To PCL	2.4E+12
To environment	7.2E+07

Figure 13 presents the temperature profile throughout the PFL. The uniform power distribution assumed in the current version of the MSDR yields a linear increase in temperature. At the core outlet, the temperature drops due to the mixing of the small amount of cold salt which passes through the reflector region. The hot salt then passes through the PFL heat exchangers and returns to the core.

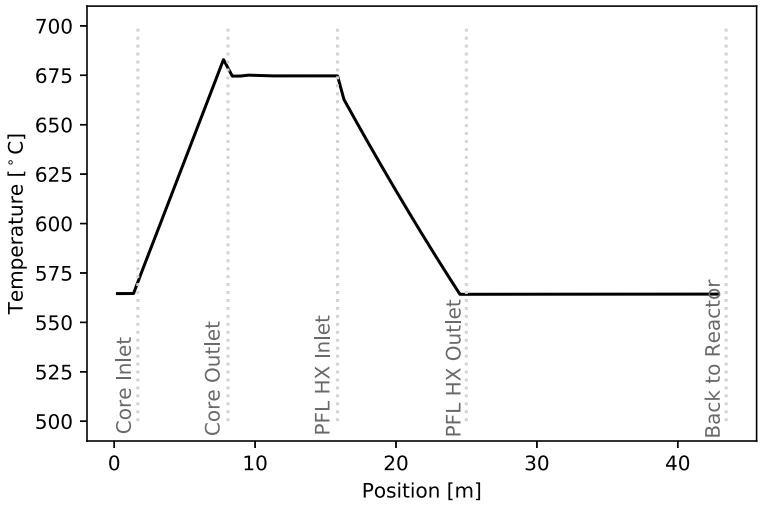

Figure 13. Steady-state temperature distribution as a function of position in the PFL.

Figure 14 presents the concentration of tritium, a selected neutron precursor group with a relatively short half-life (Group 5) and ^{135}Xe as a function of position in the reactor model. The values used for normalization are given in Table 10. The tritium in the loop decreases between the inlet of the reactor to the inlet of the core and once again from the outlet of the core to the outlet of the reactor. This decrease is due to diffusion of tritium into the graphite of the axial reflectors. These reflectors have a significant amount of surface area for transfer. The tritium builds up as the fuel salt passes through the core as a function of the power profile. The tritium decays slowly ($t_{1/2}$ = 12.3 years), so the impact from decay as it moves around the core is not noticeable in the figure. As the salt passes through the PFL heat exchangers, tritium passes through the tube walls to the PCL and ultimately to the environment. The precursor builds up in the core and then quickly decays as the salt moves through the core. Depending on the half-life of the precursor and the salt flow rate, the return concentration to the core will vary from zero to some larger, significant value. ^{135}Xe builds up in the core and decays very little as it moves around the loop ($t_{1/2}$ = 9.2 hours). However, the off-gas system is connected to the PFL at approximately 10-m. The decrease in xenon concentration that occurs due to the long hold-up period in the charcoal adsorber bed in the off-gas system can be readily observed. The pump bowl is at this position, which has the associated separation process previously described.

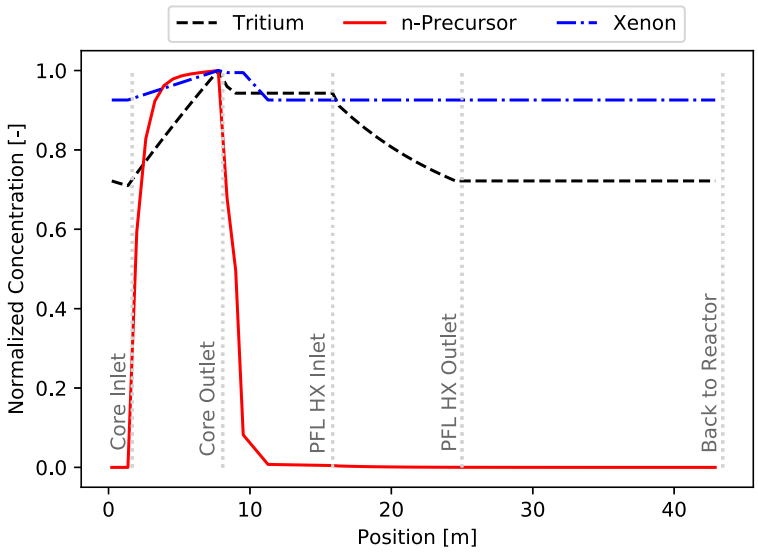

Figure 14. Steady-state normalized concentrations distribution of select precursors as a function of position in the PFL.

Table 10. Normalization values for Figure 14 (atoms/kg salt)

Variable	Value
Tritium	2.3E+13
n-Precursor	6.8E+11
Xenon	4.8E+15

V.B. Steady-State Sensitivity Analysis

The MSDR represented an immature system, compared to what would be required to construction phase, that was not optimized in many respects. This is not atypical for a design process by any means and in fact provides a point of order that a variety of sensitivity studies at various points in the design cycle are appropriate and necessary. By way of demonstration, and to better understand the impact of the system model characteristics and the input parameters on the steady-state condition of the model, a statistical analysis was performed using the Risk Analysis Virtual Environment (RAVEN)[48] and a RAVEN-Modelica interface.

Table 11 shows the selected subset of input parameters, uncertainty range, and distribution type used in this study. The parameters selected were largely associated with the kinetic behavior of the reactor, and given their importance in determining the reactor power, were selected. A few additional parameters, i.e., heat transfer coefficient correction factor, mass flow rate, and ^{135}Xe separation efficiency in the pump bowl, were selected as this are expected to have significant uncertainties in reactor design and behavior. However, the selected parameters are just a demonstration, in Modelica-based models most any parameter can be exposed for additional analysis. The sampling range was bounded by three standard deviations (3σ) to avoid unphysical values of the input parameters. Specifically, the upper and lower bounds of the input parameters were determined by *nominal value × (1±3σ)*. The only exception was ^{135}Xe separation efficiency, which was sampled between 0 and 1 while assuming a uniform distribution.

Table 11. Selected input parameters and uncertainty

Input parameter	Distribution	Sigma (σ) %	Bounds
Fraction deviation from the nominal effective delayed neutron fraction	Normal	3.0	±3σ

Fraction deviation from the nominal delayed neutron generation time	Normal	3.0	±3σ
Delayed neutron fraction (groups 1–6)	Normal	3.0	±3σ
Delayed precursor decay constant (groups 1-6)	Normal	3.0	±3σ
Absorption coefficient of fission product (e.g., ^{135}Xe)	Normal	5.0	±3σ
Fuel temperature feedback	Normal	3.0	±3σ
Graphite temperature feedback	Normal	3.0	±3σ
Correction factor on heat transfer coefficient	Normal	12.0	±3σ
Mass flow rate of primary loop	Normal	0.5	±3σ
Separation efficiency of ^{135}Xe	Uniform	-	0–1

For sampling of input parameters, the Monte Carlo sampling method was employed with a sample size of 4,000. To investigate the statistical behavior and the relationship with the input parameters shown in Table 1, five output parameters were selected: (i) total core fission power, (ii) maximum temperature of the salt in the core, (iii) maximum temperature of the graphite in the core, (iv) tritium generation rate, and (v) tritium release rate to the PCL. In Table 12, the basic statistics (i.e., mean and standard deviation) of the five output parameters are summarized. Table 12 also includes the standard errors (SE) to represent the statistical errors of the sample statistics. The SE of the sample mean was computed by Eq. (14), and the SE of the sample standard deviation (*s*) is estimated by Eq. (15).

$$SE(\overline{m}) = \sigma/\sqrt{N} \tag{14}$$

$$SE(s) = \frac{1}{2\sigma}\sqrt{\frac{1}{N}\left(\mu_4 - \frac{N-3}{N-1}\sigma^4\right)}, \tag{15}$$

where μ_4 is the fourth statistical moment computed as $\mu_4 = E(X-\mu)^4$. In Eq. (15), the population standard deviation (σ) was approximated by the sample standard deviation (*s*). It is noted that this formula is proven to be valid for any sample size and distribution.[49]

Table 12. Basic statistics for the output parameters of interest

	Nominal	**Mean ($\overline{m}$)**	**$SE(\overline{m})/\overline{m}$**	**Standard deviation (*s*)**	***SE* (*s*)**
Total fission power of the core [MWt]	724.0	658.1	0.251 %	104.5	2.13 %
Maximum temperature in the core salt [°C]	683.0	660.1	0.062 %	36.8	2.15 %

Maximum temperature in the core graphite [°C]	682.9	660.1	0.062 %	36.8	2.15 %
Tritium generation rate [atoms/s]	3.6E+16	3.3E+16	0.246 %	5.13E+15	2.17 %
Tritium release from PFL to PCL [atoms/s]	2.4E+12	1.8E+12	0.705 %	7.97E+11	1.03 %

Figure 15–Figure 17 show the distribution of the output parameters resulting from the perturbation of the input parameters, with the upper and lower 5% values (i.e., 5% percentile and 95 percentile). Figure 15 shows that the total core fission power has a skewed-left distribution (i.e., skewed with a longer tail on the left). This shape is due to the overall negative temperature feedback which prevents the core fission power from increasing excessively. This indicates the inherent safety feature of the present system. Considering that the core fission power predominantly determines the core temperature, it is natural that the similar skewed distribution is found for the maximum core salt temperature and maximum core graphite temperature, as shown in Figure 16. The same explanation can also be applied to the distribution of tritium generation rate shown in Figure 17 (left side) because the tritium generation is caused by the core fission. On the other hand, in Figure 17 (right side) the tritium release rate to the PCL is shown to have a bimodal skewed distribution, which has an additional small peak on the left tail (right side). This may be attributable to the higher density of the salt at the lower operating temperature. As the density increases, the tritium concentration (on a atoms of tritium per mass of fluid basis) can theoretically increase, causing a local maximum in concentration, and therefore, a local maximum in release rate. Naturally, this peak is bounded due to the much lower generation rate.

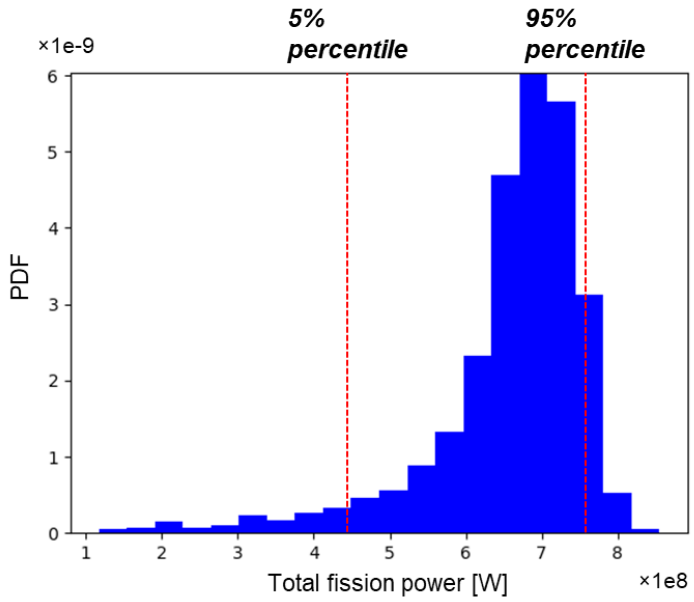

Figure 15. Distribution of fission power.

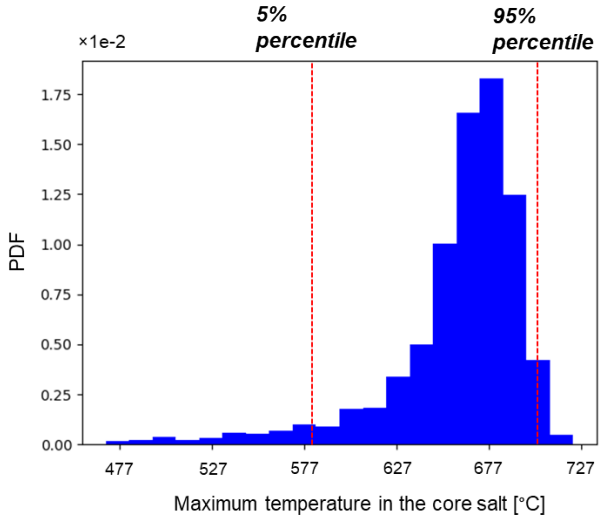

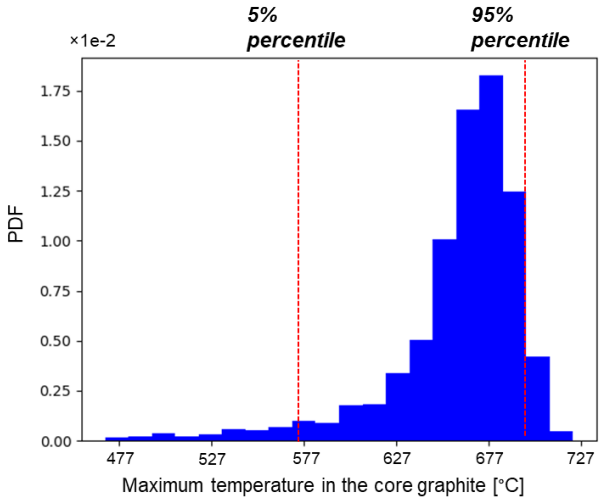

Figure 16. Distribution of maximum temperature of the core salt (left) and core graphite (right).

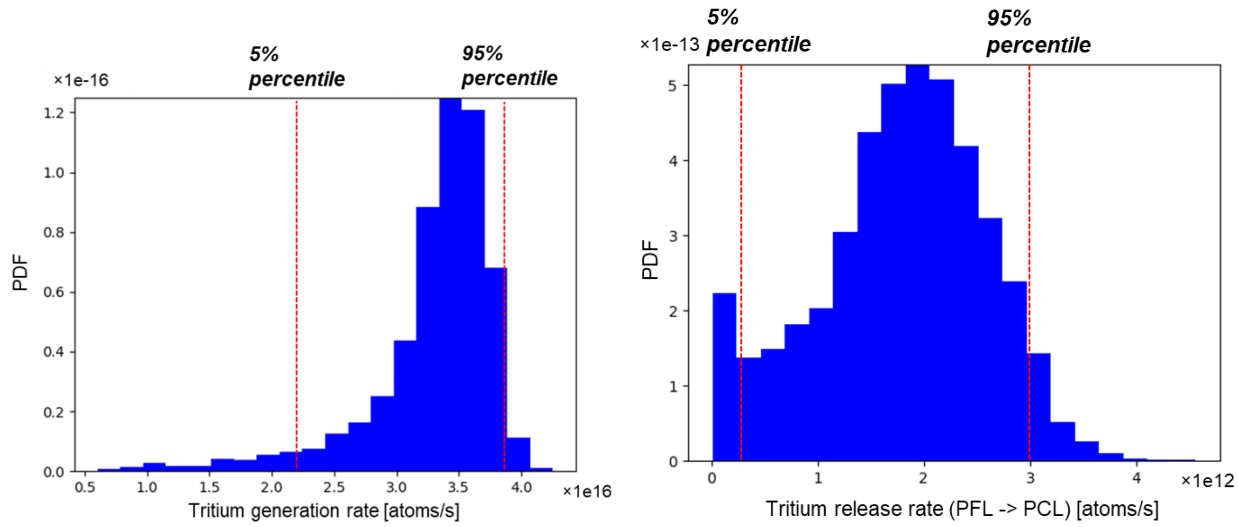

Figure 17. Distribution of tritium generation rate in the core (left) and tritium release rate to PCL (right).

In this study, the Pearson's correlation coefficient was also estimated to gain an understanding of the relationship between the selected input and output parameters. The Pearson's correlation coefficient is a test statistic to measure the statistical relationship between the two variables.[50] To determine whether the relationship is statistically significant, a statistical hypothesis test was employed, along with the estimated values of Pearson's correlation coefficients. Specifically, the two-tailed *t*-test was performed with a null hypothesis stating that "there is no statistical relationship between the two parameters." To implement this approach, the *t*-statistic (*t*) must be calculated as shown in Eq. (16), where r is the correlation coefficient.

$$t = r\sqrt{\frac{N-2}{1-r^2}} \tag{16}$$

Once sample size *N* and significance level α are known, the critical *t*-value (t_{crit}) can be determined from the *t*-table or by using the statistical software. Then, using the critical *t*-value and sample size *N*, the critical value of the correlation coefficient, r_{crit}, can be obtained from Eq. (16). Finally, this r_{crit} can be used to evaluate the statistical significance of Pearson's correlation coefficient. The null hypothesis will be rejected if $t>t_{crit}$ (*i.e.*, statistically significant); otherwise, the null hypothesis will not be rejected (*i.e.*, statistically insignificant).

With the sample size N=4000 and significance level α=0.05, the critical values, t_{crit} and $r_{crit,}$ were estimated to be 1.961 and 0.031, respectively. Based on these values, the statistical relationship between the input and output parameters can be argued at the 95 % confidence level. Table 13 shows the input parameters which were determined to have a significant impact on the output parameters of present interest. That is, the estimated Pearson's correlation coefficients for these inputs were larger than the critical value (i.e., $t>t_{crit}$=0.031). Table 13 also shows that the ^{135}Xe separation efficiency has the greatest impact on all the output parameters. This impact can also be seen in Figure 18, which is the 3D plot presenting the variation of tritium release rate to PCL against the effective delayed neutron deviation fraction and ^{135}Xe separation efficiency. It is clear from Figure 18 that the tritium release rate to PCL is impacted more significantly by the ^{135}Xe separation efficiency. The large impact of ^{135}Xe separation efficiency is a result of the large absorption cross section and the associated impact on reactivity caused by having more, or less, ^{135}Xe in the PFL.

It is noted that the key input parameters can be selected and prioritized in this way for any subsequent uncertainty analysis. More generally, the presented analysis helps to reduce the complex nature of the model to actionable items. Depending on the analysis ran, the results can inform on a range of issues such as on portions of the model that need to have their uncertainty reduced (e.g., heat transfer coefficients) due to their importance in the output parameters of interest or in detecting phenomena that is, or is not, present and should, or should not be, thereby providing insight to the modeler on if there are gross errors in the assumptions made in the model. Expanded analysis such as this in tandem with modeling and design iterations is an important part of advancing the state-of-the-art and will be an ongoing portion of future work.

Table 13. Pearson's correlation coefficient

	Total core fission power	**T_{max} of the core salt**	**T_{max} of the core graphite**	**Tritium generation rate**	**Tritium release from PFL to PCL**
Effective delayed neutron fraction	-0.205	-0.207	-0.207	-0.202	-0.314
Delayed neutron fraction (group 2)	0.060	0.058	0.058	0.060	0.087
Delayed neutron fraction (group 3)	0.041	0.042	0.042	0.041	0.065
Delayed neutron fraction (group 4)	0.228	0.227	0.227	0.225	0.347
Delayed neutron fraction (group 5)	0.076	0.078	0.078	0.075	0.116

Delayed neutron fraction (group 6)	0.028	0.027	0.027	0.028	0.043
Delayed precursor decay constant (group 2)	0.011	0.011	0.011	0.010	0.039
Delayed precursor decay constant (group 3)	0.041	0.040	0.040	0.040	0.067
Delayed precursor decay constant (group 4)	0.094	0.095	0.095	0.094	0.119
Absorption coefficient of fission product (e.g., ^{135}Xe)	-0.034	-0.035	-0.035	-0.034	-0.036
Fuel temperature feedback	0.111	0.111	0.111	0.110	0.144
Graphite temperature feedback	-0.082	-0.083	-0.083	-0.082	-0.096
Correction factor on heat transfer coefficient	0.093	0.012	0.012	0.095	0.151
Mass flow rate of primary loop	-0.026	-0.037	-0.037	-0.025	-0.027
Separation efficiency of ^{135}Xe	0.685	0.687	0.687	0.682	0.718

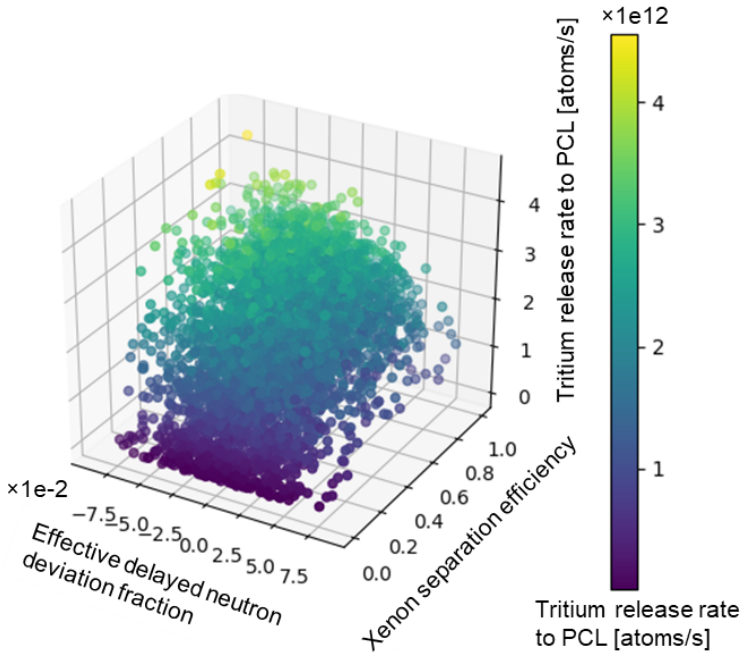

Figure 18. Multidimensional (3D) statistical analysis

V.C. Transient Events: PFL Pump Trip with and without Control Rod Action

As a reminder, in the presented model the BOP is fixed inlet mass flow rate and temperature and fixed outlet pressure. Furthermore, the following scenarios exercise the model and are not necessarily

appropriate for deriving broad conclusions about MSR behavior. Variations in the system model (e.g., lengths, volumes, and rod insertion rates) will change results/conclusions though a more exhaustive study might reveal more items of interest. Pairing this type of scenario investigation with a sensitivity analysis like that performed on the steady-state results or frequency response analysis[51] is a proposed path forward and will be pursued in future work.

The transient cases performed simulated various combinations of PFL pump trips with and without control rod action. Table 14 provides a brief description of each of the scenarios and scenario labels for reference. As appropriate, per the scenario description, the pump flow rate was exponentially decreased with a decay constant (λ) with the initial values of all system variables based on the steady-state values at 172,800 seconds (zero-time in the Figures 19 - 24) and an offset of 0.1% of the nominal steady-state flow rate. The small amount of flow rate was permitted to avoid any potential numerical issues associated with zero flow. For cases with control rod action, negative reactivity of different amounts (ρ_{CR}) was inserted at a constant rate of ~1.5 inches per second (i.e., 150 seconds to fully insert an 18 ft. control rod).

Table 14. Scenario description

Scenario	λ (s^{-1})	ρ_{CR} (pcm)
A	1/40	0
B	1/20	0
C	1/40	-300
D	1/40	-3,000

The overall temperature feedback of the modeled MSR is negative, though not overly negative due to significant positive reactivity feedback from the graphite. Therefore, as the mass flow rate decreases (Figure 19), it causes the reactor fission power to decrease proportionally over time (Figure 20) as the kinetics of the reactor strive to correct the imbalance from the reference temperature state. Less flow increases the temperature of the reactor, which adds negative reactivity feedback to the power kinetics (Figure 21). The hump in decay heat within the core is likely attributable to short-lived decay products that were decaying in other portions of the PFL but are now decaying in the core due the decreased flow of salt. Depending on the amount reactivity and its insertion rate, the final temperature of the core may increase or decrease from the nominal value (Figure 22).

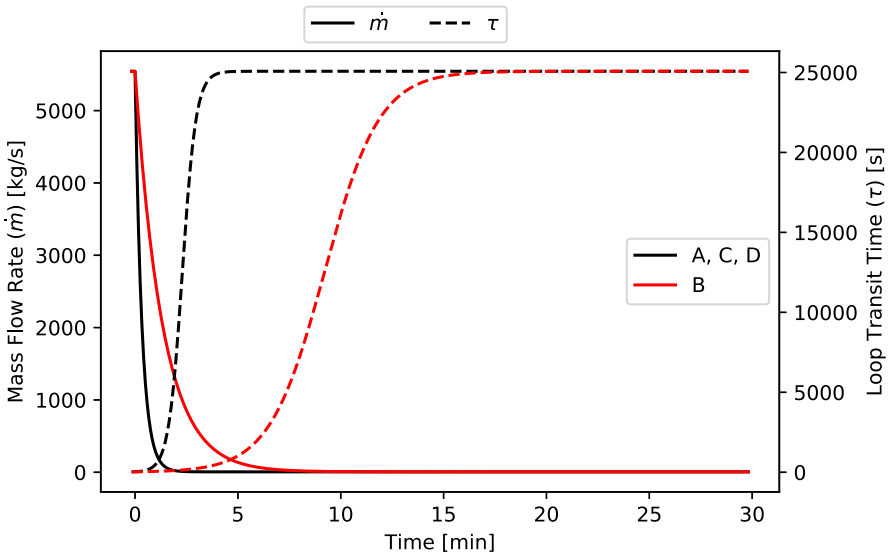

Figure 19. Mass flow rate and loop transit time as a function of time.

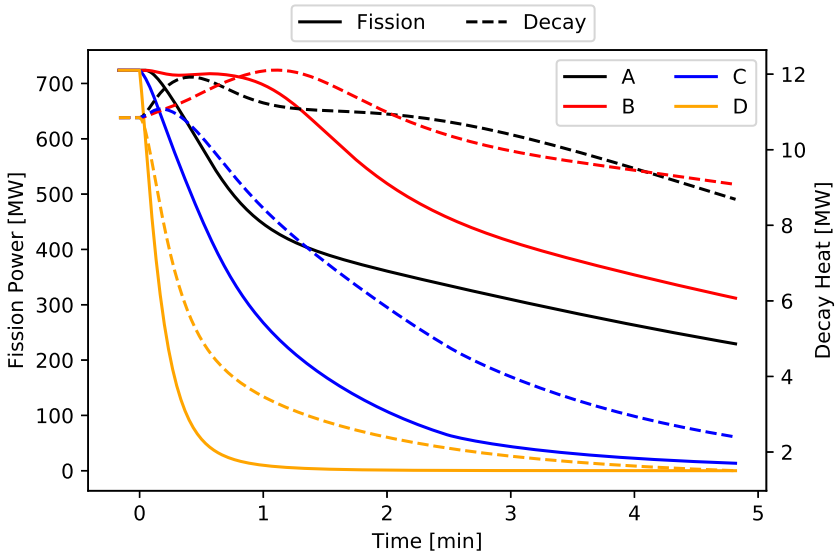

Figure 20. Fission and in-core decay heat as a function of time.

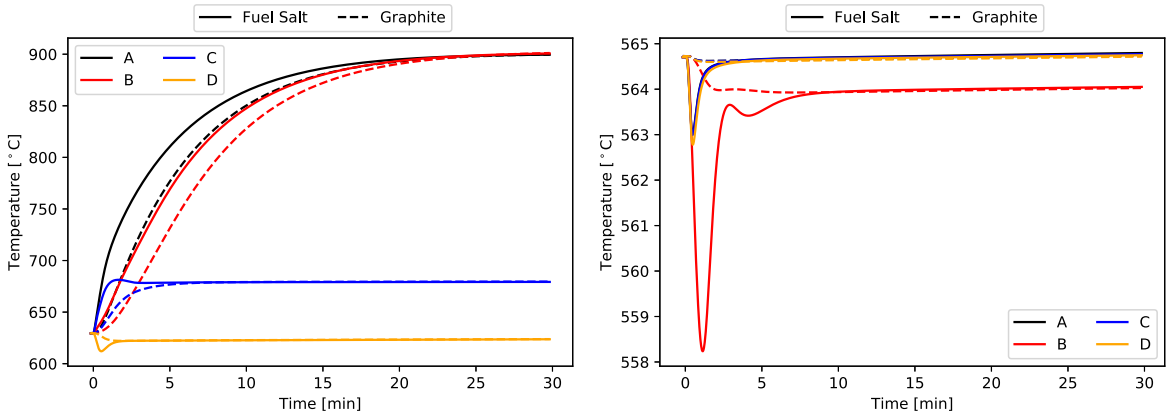

Figure 21. Average temperature of fuel salt and graphite for the core (left) and radial reflector (right).

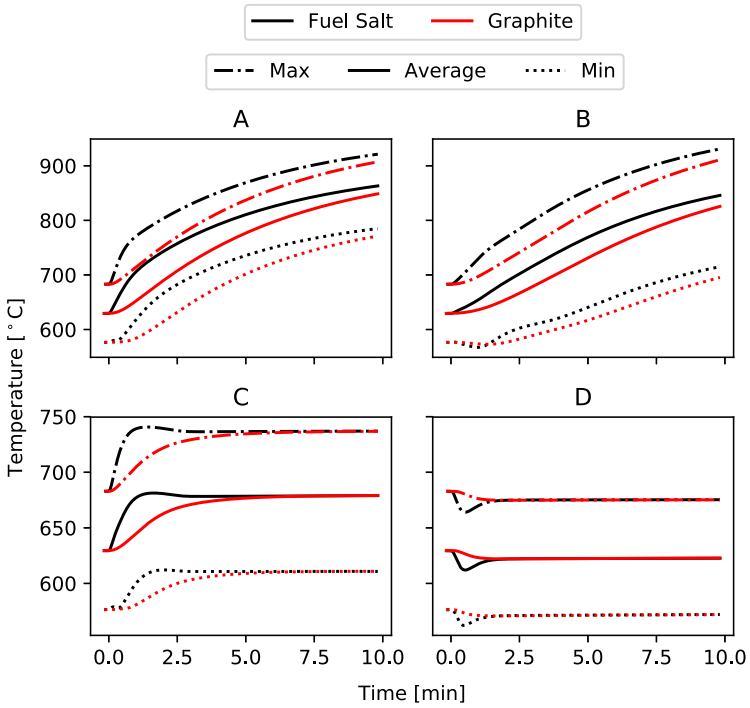

Figure 22. Maximum, average, and minimum fuel and graphite temperatures in the core.

Figure 23 demonstrates the normalized rate of tritium release from the system. The normalization value is for the rates at steady-state shown in Table 9. The generation rate of tritium tracks the fission power. The flow rate of the PFL sets the concentration gradient and diffusion coefficient at the PHX of tritium and therefore sets the rate of transfer between the PFL and PCL, “To PCL” in Fig. 23. Therefore,

tritium transfer decreases in accordance with the PFL flow rate. However, the release to the environment changes little directly due to flow rate changes in the PFL. Instead, concentration gradient changes and solubility changes due to shift in temperatures drive the small bump in each scenario's release of tritium to the environment.

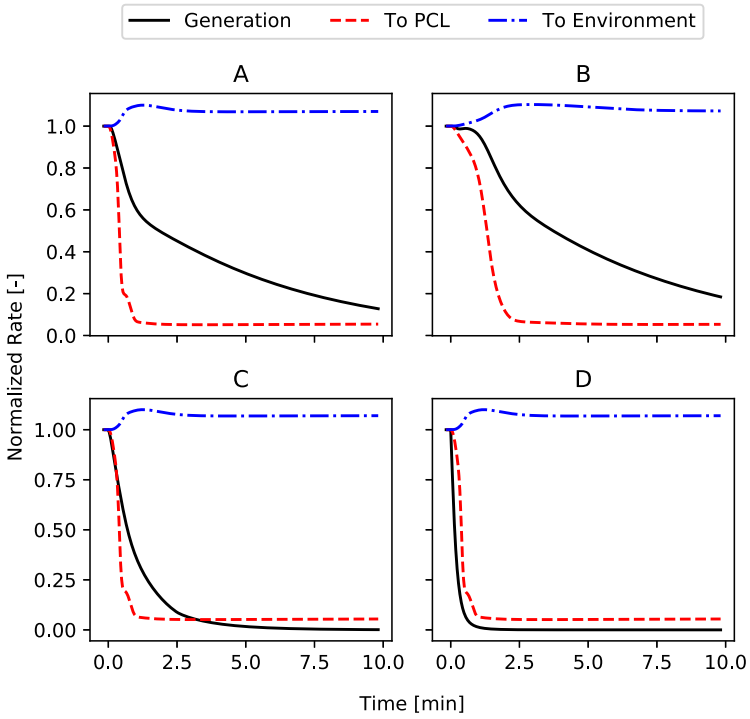

Figure 23. Normalized tritium generation and release rate as a function of time.

Figure 24 provides surface plots for scenario A as a function of time and position in the loop. For this report, these plots are more demonstrative of general trends and capability and therefore are limited to scenario A. Additional plots for each scenario can be found in Greenwood et al.[13] These plots enhance understanding of the overall behavior of the loop over a transient event. The changes in temperatures, concentrations, etc., discussed above hold true, such as the rise in core temperature and impact of decrease in tritium generation, and they can be examined spatially to clarify the scenario over time. The concentration plots illustrate the change in tritium, neutron precursor group 5, and ^{135}Xe concentration on a salt mass basis. The neutron precursor group 5 is a short-lived precursor. Therefore, the plot demonstrates that these types of transients have little impact on group 5's behavior as it decays away so quickly. When the reactor shuts down, regardless of the scenario, the ^{135}Xe concentration builds up over

time due to the decay of iodine. In the figure, the ^{135}Xe concentration has just barely reached a maximum and is starting to diminish due to iodine having decayed to low levels and ^{135}Xe decay becoming the dominating factor in the ^{135}Xe balance.

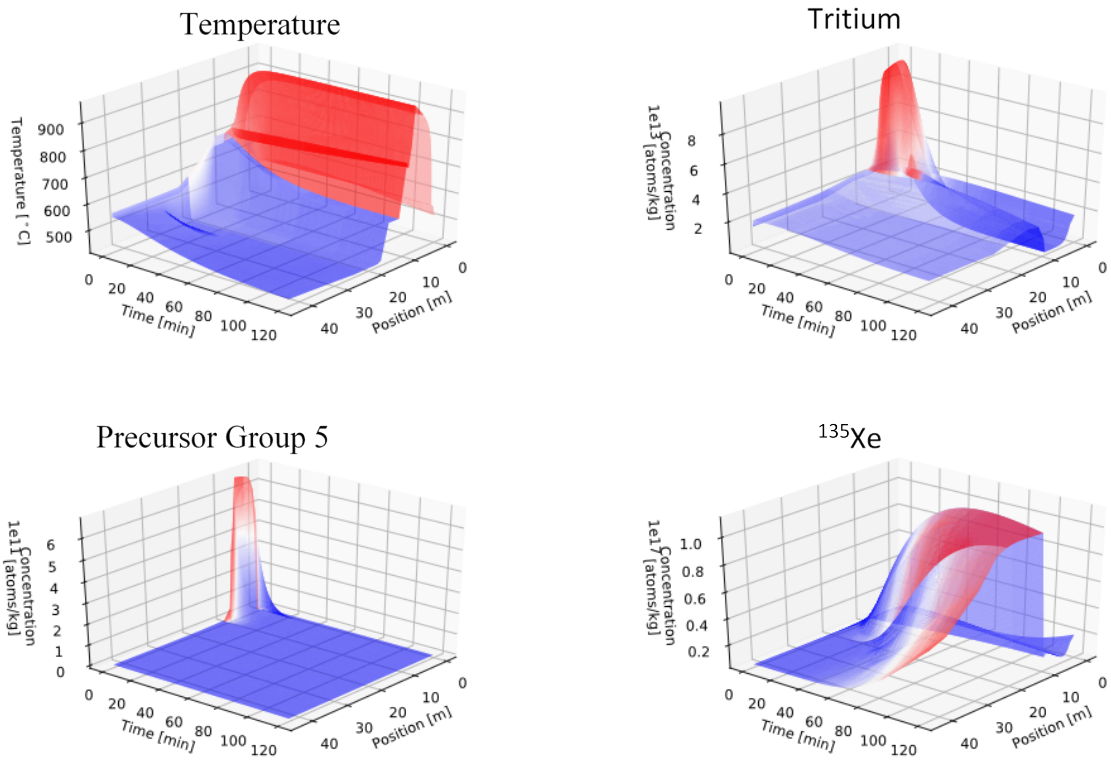

Figure 24. Scenario A temperature and tritium, neutron precursor group 5, and ^{135}Xe concentration as a function of time and position.

VI. Conclusions

This work outlines capabilities needed from MSR system modeling tools via identification of criteria derived from several key areas. These areas include licensing and safeguards, ability to model the breadth of phenomena and systems needing to be understood in MSRs, and expectation that the MSR community needs very near-term tools to advance their work. Near term tools will also help accelerate development of future tools which will ultimately provide the safety basis for licensing. The identification of this criteria is then followed by the presentation of TRANSFORM, an ORNL developed,

Modelica-based dynamic system modeling tool which will assist in bridging the gap in advanced reactor modeling and simulation. Using the MSDR as a surrogate reactor concept of the class of liquid-fueled designs currently being pursued by the advanced reactor community, a demonstration of TRANSFORM capabilities is presented using various steady state and transient scenarios, including sensitivity analysis of the steady state behavior using the advanced modeling framework RAVEN.

The modeling approach and capabilities integrated into the TRANSFORM-Modelica model of the MSDR were largely driven by criteria derived from several author proposed questions related to licensing and safeguards needs. Each of these criteria were met in the creation of this model and have been implemented in generic fashion using a component-based approach that allows for future reactor-specific, or scenario of interest, modifications. In particular, the integration of the birth, decay, and transport of fission products throughout the reactor system with the thermal hydraulics system, using quantifiable tracking approaches, as opposed to other approaches such as time constants, is incorporated in the model. The capabilities demonstrated by in this paper provide a means to develop a more complete understanding of the complex behavior of liquid-fueled MSRs from both safety-related licensing and mass accountancy safeguards perspectives and from an agile development workflow, critical to advancing MSRs to commercial deployment.

TRANSFORM allows for rapid prototyping and allows the modeler to incorporate new physics and features as needed. Furthermore, the open nature of the Modelica language provides new opportunities for code coupling and advanced workflow integration. Integration of TRANSFORM with other advanced tools and workflows such as RAVEN is a key aspect of advancing the modeling and simulation of MSRs and critical to closing the gap between where the community stands and what it seeks to achieve in the future.

VI.A. Future Work

To continue to advance the modeling capabilities of advanced tools and move forward reactor design and analysis needs, a variety of future tasks will be undertaken. This includes modeling tasks to introduce additional components/physics into the TRANSFORM Library such as 1D multigroup diffusion models, additional chemistry processes (e.g., corrosion, tritium chemistry, and redox potential) other pertinent auxiliary systems not typically permitted to be modeled in nuclear system codes, use of salt

chemistry databases for fluid property determination once available (including additional transmutation and burnup impacts), and continued demonstration of coupling with other advance tools like RAVEN (e.g., ORIGIN, STAR-CCM+, etc.).

Additional analysis tasks include enabling advanced workflows to assist modelers in gaining a better understanding of the complex behaviors of their systems. Tasks include generation of clear methodologies for performing sensitivity analysis and parameter significance ranking, stability and other frequency response analysis methods, model calibration, and code-to-code or code-to-experiment comparisons workflows. Fortunately, a variety of excellent tools are available that provide many of the capabilities needed to perform analyses such as those mentioned. The task is then reduced to generating the workflows that link the analysis tools with the dynamic models, which, coupled with the ability of Modelica-based models to interface with external tools (e.g., FMI), is achievable in the near term.

Acknowledgments

This research was funded by the US Department of Energy's Office of Advanced Reactor Technology Molten Salt Reactor Campaign.

References

1. Yacobucci, B. D. *Energy Policy: 114th Congress Issues*. 11 (Congressional Research Service, 2016).

2. Rosenthal, M. W., Kasten, P. R. & Briggs, R. B. Molten-Salt Reactors. History, Status, and Potential. *Nucl. Appl. Technol.* **8**, 107–117 (1970).

3. Krahn, S. *et al.* Why Reconsider a Molten Salt Reactor? in *Transactions of the American Nuclear Society* **111**, (American Nuclear Society, 2014).

4. Ingersoll, D. T. & Forsberg, C. W. *Status of Preconceptual Design of the Advanced High-Temperature Reactor (AHTR)*. (Oak Ridge National Lab. (ORNL), Oak Ridge, TN (United States), 2004).

5. Ingersoll, D. T. *Status of Physics and Safety Analyses for the Liquid-Salt-Cooled Very High-Temperature Reactor (LS-VHTR)*. (Oak Ridge National Lab. (ORNL), Oak Ridge, TN (United States), 2005).

6. Ingersoll, D. T., Forsberg, C. W. & MacDonald, P. E. *Trade Studies for the Liquid-Salt-Cooled Very High-Temperature Reactor: Fiscal Year 2006 Progress Report*. (Oak Ridge National Lab. (ORNL), Oak Ridge, TN (United States), 2007).

7. Qualls, A. L. *et al. Fluoride Salt-Cooled High-Temperature Demonstration Reactor Point Design*. (Oak Ridge National Laboratory (ORNL), Oak Ridge, TN (United States), 2016). doi:10.2172/1245361

8. Qualls, A. L. *et al.* Preconceptual design of a fluoride high temperature salt-cooled engineering demonstration reactor: Motivation and overview. *Ann. Nucl. Energy* **107**, 144–155 (2017).

9. Brown, N. R. *et al.* Preconceptual design of a fluoride high temperature salt-cooled engineering demonstration reactor: Core design and safety analysis. *Ann. Nucl. Energy* **103**, 49–59 (2017).

10. Software Technology Support Center Cost Analysis Group. *Software Development Cost Estimating Guidebook*. 254 (Price Systems, LLC, 2009).

11. NEAMS. *NEAMS: The Nuclear Energy Advanced Modeling and Simulation Program*. (Nuclear Energy Advanced Modeling and Simulation Program, 2013).

12. Mesina, G. L. A History of RELAP Computer Codes. *Nucl. Sci. Eng.* **182**, v–ix (2016).

13. Greenwood, M. S., Betzler, B. R. & Qualls, A. L. *Dynamic System Models for Informing Licensing and Safeguards Investigations of Molten Salt Reactors*. (Oak Ridge National Lab. (ORNL), Oak Ridge, TN (United States), 2018). doi:10.2172/1456790

14. NRC. *Nuclear Power Plant Licensing Process Fact Sheet*. (Nuclear Regulatory Commission, 2010).

15. Bajorek, S. & Diamond, D. J. *Thermal-Hydraulics Phenomena Important in Modeling and Simulation of Liquid-Fuel Molten Salt Reactors*. (Brookhaven National Laboratory (BNL), Upton, NY (United States), 2018).

16. Betzler, B. R. (ORCID:0000000184259711) *et al. Molten Salt Reactor Campaign Modeling and Simulation Program Plan*. (Oak Ridge National Lab. (ORNL), Oak Ridge, TN (United States), 2018). doi:10.2172/1480625

17. IAEA. *The Structure and Content of Agreements Between the Agency and States Required in Connection with the Treaty on the Non-Proliferation of Nuclear Weapons*. (International Atomic Energy Agency, 1972).

18. Agile Alliance. Manifesto for Agile Software Development. (2001). Available at: http://agilemanifesto.org/. (Accessed: 18th April 2019)

19. Agile Alliance. Principles behind the Agile Manifesto. (2001). Available at: http://agilemanifesto.org/principles.html. (Accessed: 18th April 2019)

20. Diamond, D. J., Brown, N. R., Denning, R. & Bajorek, S. *Phenomena Important in Molten Salt Reactor Simulations*. (Brookhaven National Laboratory (BNL), Upton, NY (United States), 2018). doi:10.2172/1436452

21. Diamond, D. J. *Neutronics Phenomena Important in Modeling and Simulation of Liquid-Fuel Molten Salt Reactors*. (Brookhaven National Laboratory (BNL), Upton, NY (United States), 2018).

22. Brinton, S. *The Advanced Nuclear Industry*. (Third Way, 2015).

23. ORNL-TRANSFORM. TRANSFORM-Library: A Modelica Library of Multi-Physics Components. (2017). Available at: https://github.com/ORNL-TRANSFORM/TRANSFORM-Library. (Accessed: 22nd August 2017)

24. Dassault Systemes. Dymola Systems Engineering. Available at: https://www.3ds.com/products-services/catia/products/dymola/. (Accessed: 16th August 2017)

25. Modelica Association. Modelica Language Specification Version 3.4. (2017).

26. Hale, R. *et al. Update on ORNL TRANSFORM Tool: Preliminary Architecture/Modules for High-Temperature Gas-Cooled Reactor Concepts and Update on ALMR Control*. (Oak Ridge National Laboratory (ORNL), Oak Ridge, TN (United States), 2015).

27. Greenwood, M. S. Component Development for Nuclear Hybrid Energy Systems. in 839–846 (2017). doi:10.3384/ecp17132839

28. Rabiti, C. *et al. Status Report on Modelling and Simulation Capabilities for Nuclear-Renewable Hybrid Energy Systems*. (Idaho National Laboratory, 2017).

29. Rader, J. D., Greenwood, M. S., Wysocki, A. J., Poore, W. P. & Melin, A. M. *SMR-160 Primary Flow Stability*. (Oak Ridge National Laboratory, Oak Ridge, TN (United States), 2018).

30. Rader, J. D., Smith, M. B. R., Greenwood, M. S. & Harrison, T. J. Nuclear Thermal Propulsion Dynamic Modeling with Modelica. in *Proceeding of Nuclear and Emerging Technologies for Space (NETS)* (2019).

31. Modelica Association. Modelica and the Modelica Association. Available at: https://www.modelica.org/. (Accessed: 16th August 2017)

32. Functional Mock-up Interface. Available at: http://fmi-standard.org/. (Accessed: 23rd February 2018)

33. Pop, A., Östlund, P., Casella, F., Sjölund, M. & Franke, R. A New OpenModelica Compiler High Performance Frontend. in 689–698 (2019). doi:10.3384/ecp19157689

34. Modelica Association. *Modelica Standard Library*. (Modelica Association, 2018).

35. Casella, F., Otter, M., Proelss, K., Richter, C. & Tummescheit, H. The Modelica Fluid and Media Library for Modeling of Incompressible and Compressible Thermo-Fluid Pipe Networks. 10 (2006).

36. Greenwood, M. S. & Betzler, B. R. Modified Point-Kinetics Model for Neutron Precursors and Fission Product Behavior for Fluid-Fueled Molten Salt Reactors. *Nucl. Sci. Eng.* 1–14 (2018). doi:10.1080/00295639.2018.1531619

37. Bettis, E. S., Alexander, L. G. & Watts, H. L. *Design Studies of a Molten-Salt Reactor Demonstration Plant*. (1972).

38. Robertson, R. C. *Conceptual Design Study of a Single-Fluid Molten-Salt Breeder Reactor*. (Oak Ridge National Laboratory, 1971).

39. Betzler, B. R., Powers, J. J. & Worrall, A. Molten salt reactor neutronics and fuel cycle modeling and simulation with SCALE. *Ann. Nucl. Energy* **101**, 489–503 (2017).

40. Chadwick, M. B. *et al.* ENDF/B-VII.1 Nuclear Data for Science and Technology: Cross Sections, Covariances, Fission Product Yields and Decay Data. *Nucl. Data Sheets* **112**, 2887–2996 (2011).

41. Stempien, J. D. Tritium Transport, Corrosion, and Fuel Performance Modeling in the Fluoride Salt-Cooled High-Temperature Reactor (FHR). (Massachusetts Institute of Technology, 2015).

42. Mays, G. T., Smith, A. N. & Engel, J. R. *Distribution and Behavior of Tritium in the Coolant-Salt Technology Facility*. (Oak Ridge National Lab. (ORNL), Oak Ridge, TN (United States), 1977).

43. Rader, J. D., Greenwood, M. S. & Humrickhouse, P. W. Verification of Modelica-Based Models with Analytical Solutions for Tritium Diffusion. *Nucl. Technol.* 1–8 (2018). doi:10.1080/00295450.2018.1431505

44. Olander, D. Redox Condition in Molten Fluoride Salts. *J. Nucl. Mater.* **300**, 270–272 (2002).

45. Zeng, Y. *et al.* Development of the Tritium Transport Analysis Code for the Thorium-Based Molten Salt Reactor. *Nucl. Technol.* **203**, 48–57 (2018).

46. Sun, C. L. *et al.* Dynamic adsorption properties of Kr and Xe isotopes in charcoal. *J. Radioanal. Nucl. Chem.* **181**, 291–299 (1994).

47. McMurray, J. *et al. Multi-physics Simulations for Molten Salt Reactor Evaluation: Chemistry Modeling and Database Development*. (Oak Ridge National Lab. (ORNL), Oak Ridge, TN (United States), 2018).

48. Rabiti, C. *RAVEN: Risk Analysis Virtual Environment*. (Idaho National Laboratory, 2018).

49. Rao, C. R. *Linear Statistical Inference and its Applications*. (Wiley, 2002).

50. Alfonsi, A. *et al. RAVEN Theory Manual*. (2016). doi:10.2172/1260312

51. Ball, S. J. & Kerlin, T. W. *Stability Analysis of the Molten-Salt Reactor Experiment*. (Oak Ridge National Lab., Tenn., 1965).